

Squaramide based ion pair receptors possessing ferrocene as a signaling unit

Marta Zaleskaya, Damian Jaglencic, Marcin Karbarz, Łukasz Dobrzycki, Jan Romański

Table of Contents

1. ^1H and ^{13}C NMR SPECTRA	1
2. UV-vis titration experiments	7
2.1. Dilution plots	8
2.2. Job Plots	9
2.3. Binding isotherms	10
3. NMR Titration	21
4. Electrochemical measurements	26
5. X-Ray crystallographic data	26
5.1. References Supplementary	30

1. ^1H and ^{13}C NMR SPECTRA

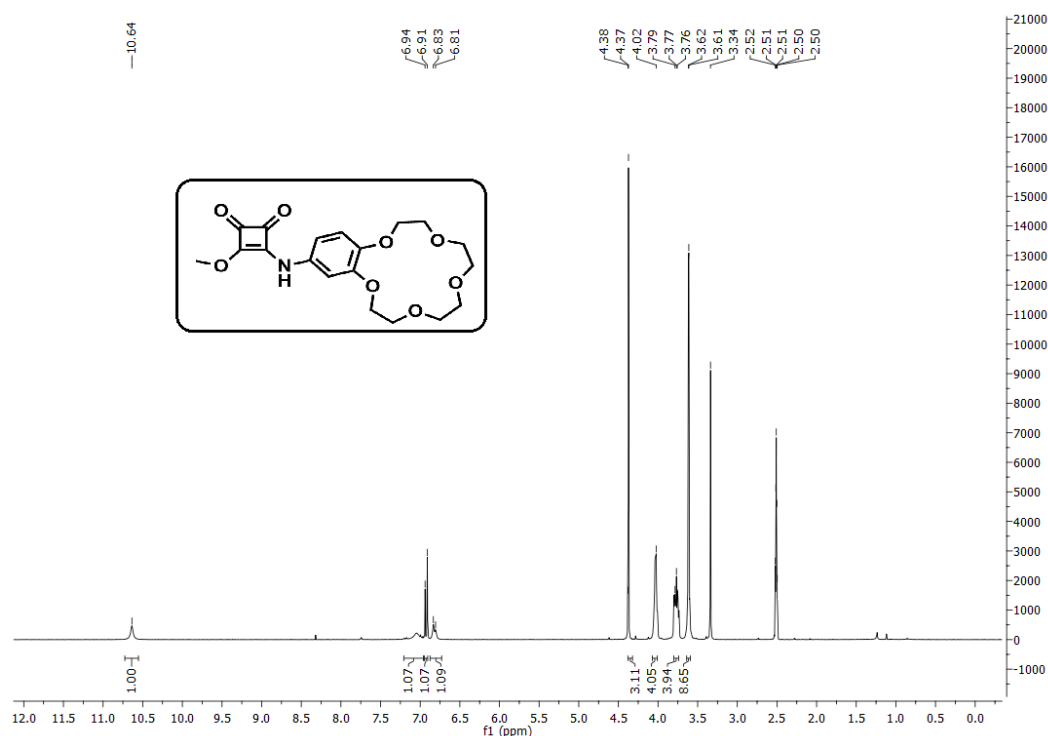


Fig. S1: ^1H NMR spectrum of compound **4a** in DMSO.

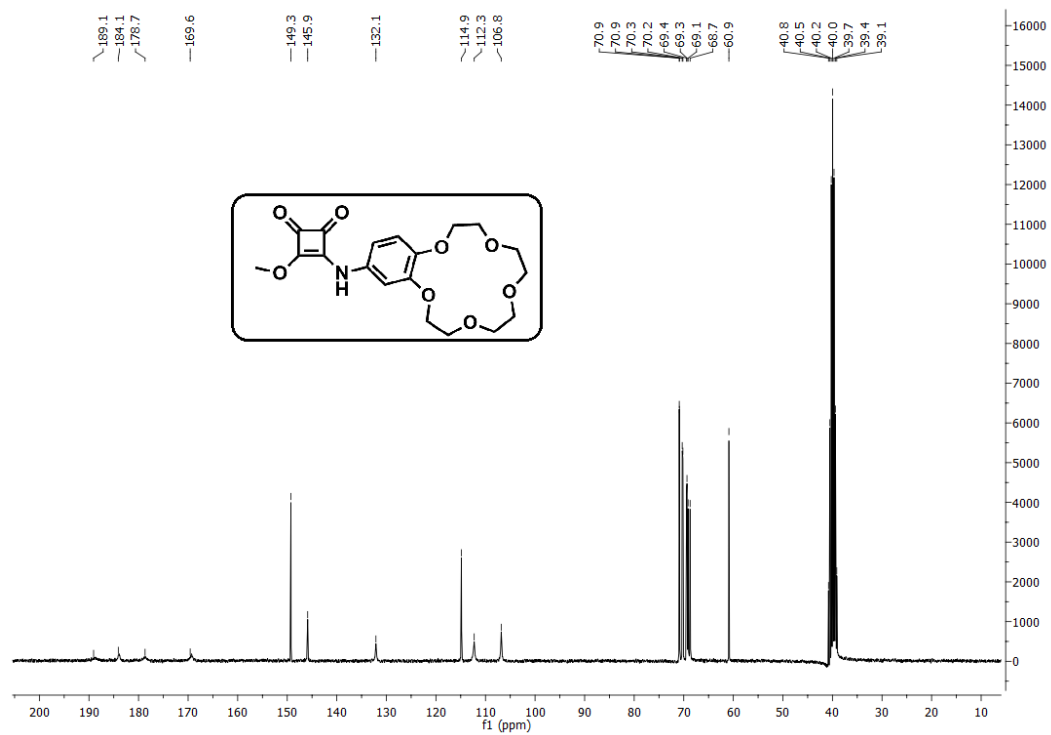


Fig. S2: ^{13}C NMR spectrum of compound 4a in DMSO.

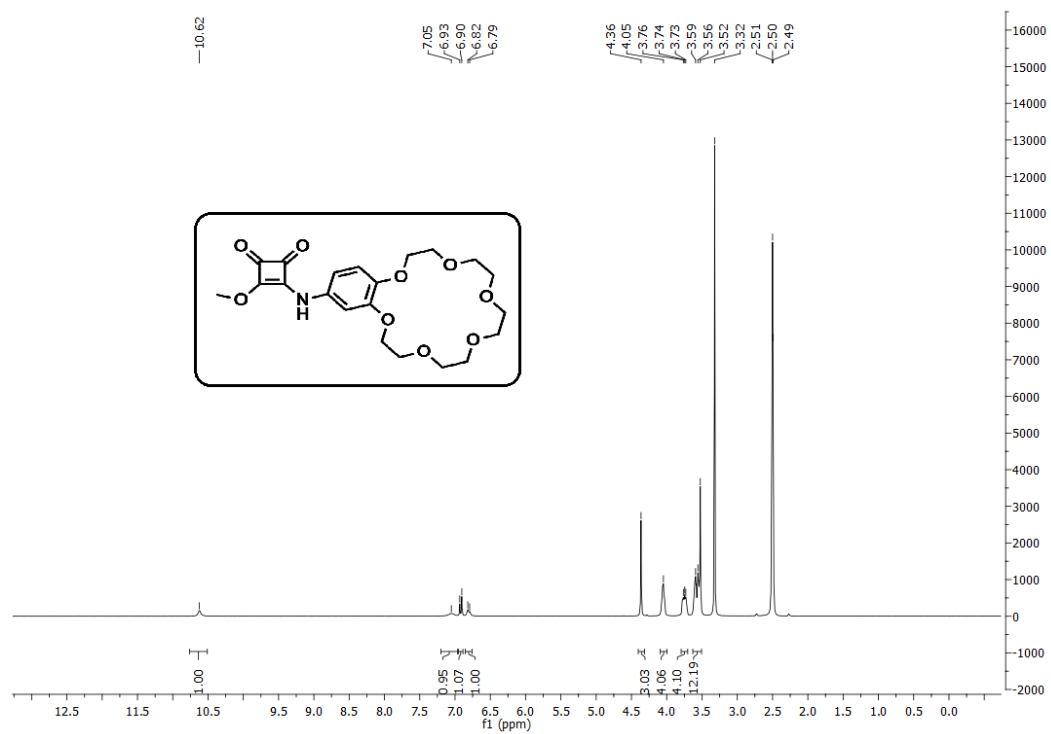


Fig. S3: ^1H NMR spectrum of compound 4b in DMSO.

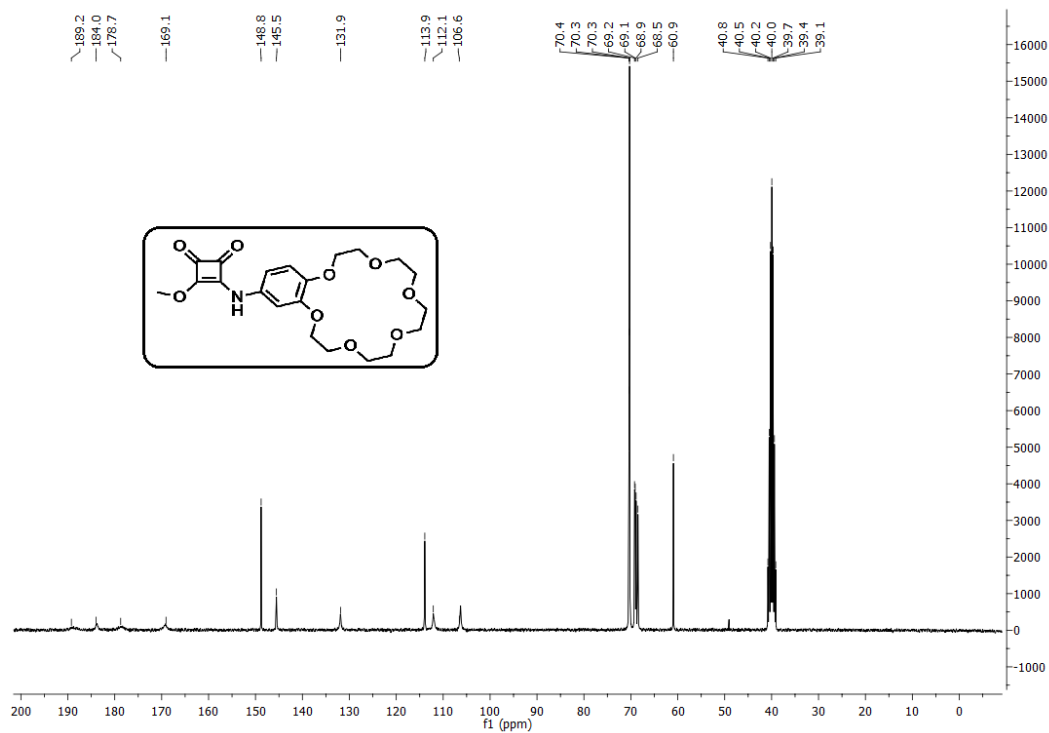


Fig. S4: ^{13}C NMR spectrum of compound **4b** in DMSO.

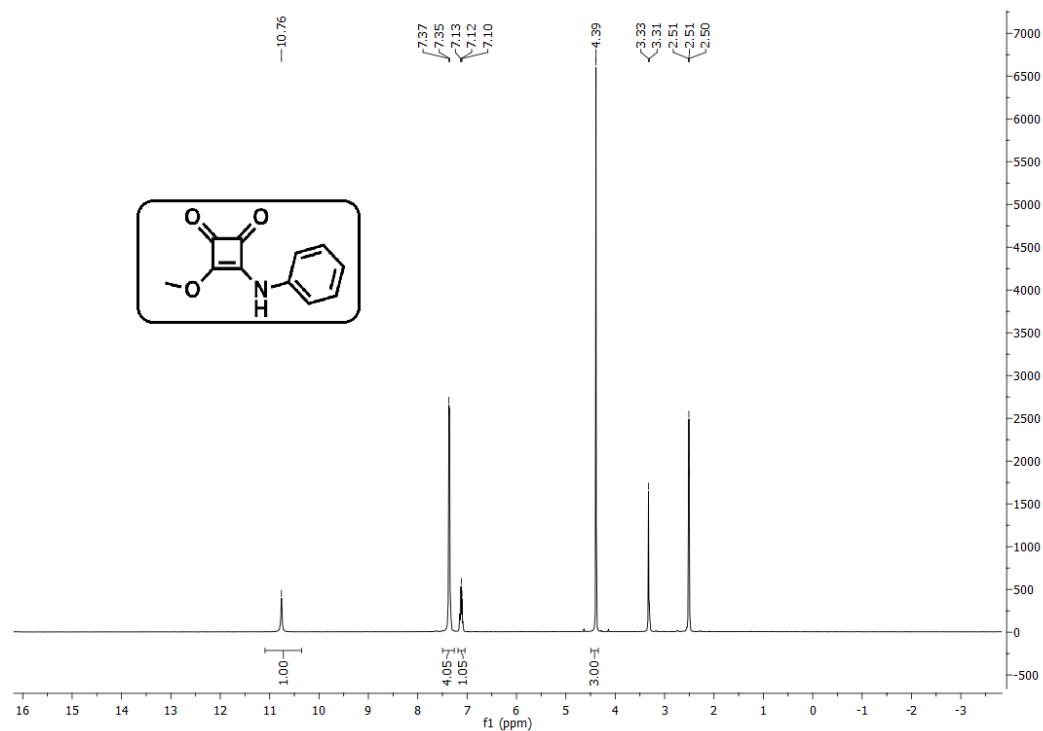


Fig. S5: ^1H NMR spectrum of compound **5** in DMSO.

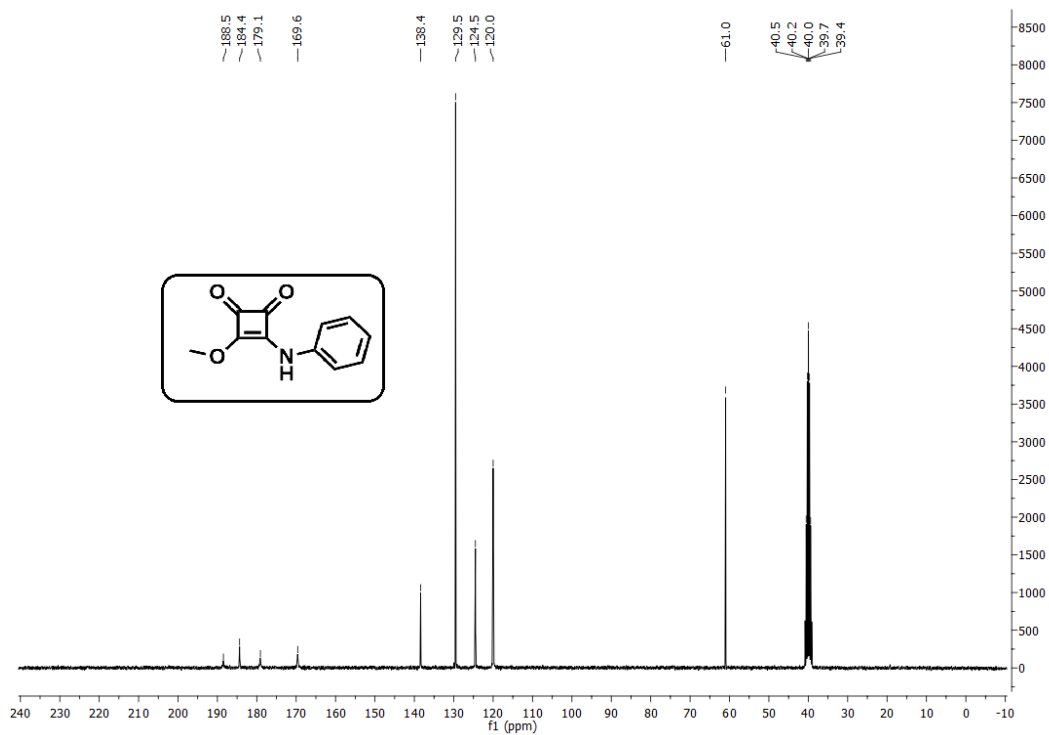


Fig. S6: ^{13}C NMR spectrum of compound 5 in DMSO.

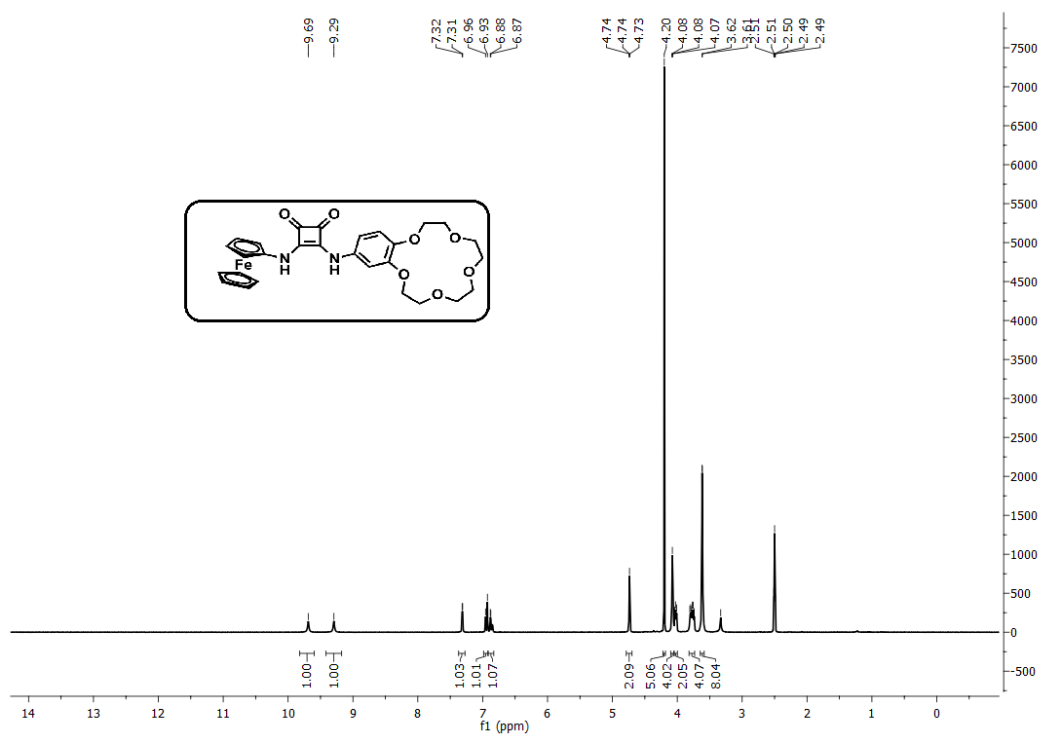


Fig. S7: ^1H NMR spectrum of receptor 1 in DMSO.

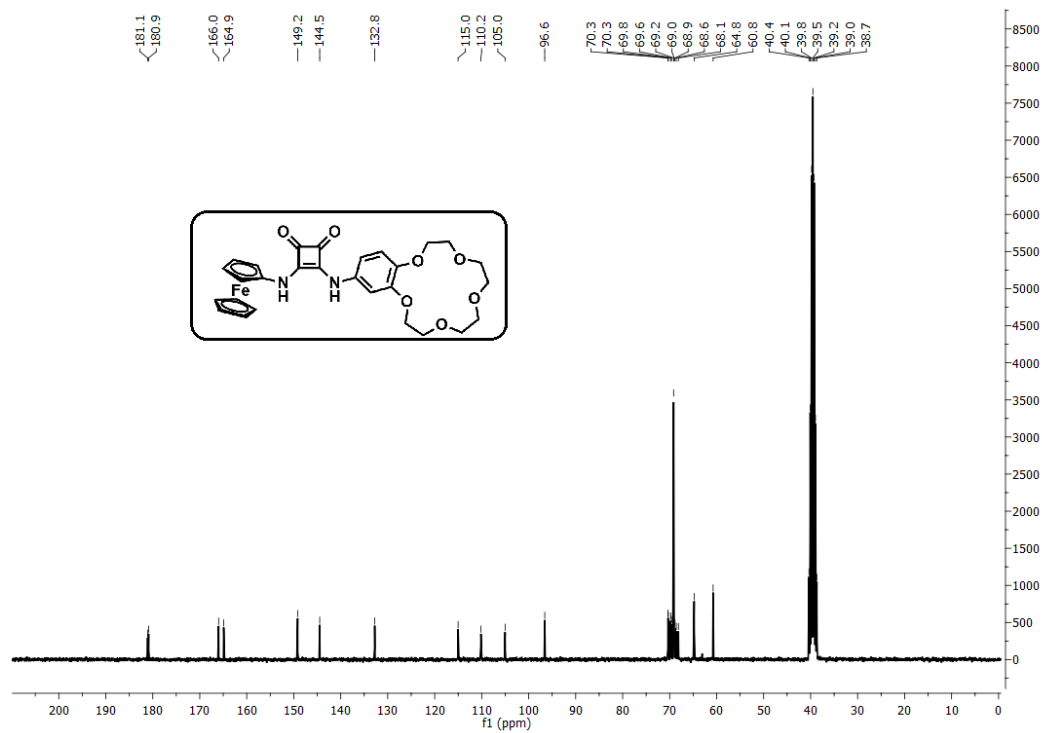


Fig. S8: ^{13}C NMR spectrum of receptor **1** in DMSO.

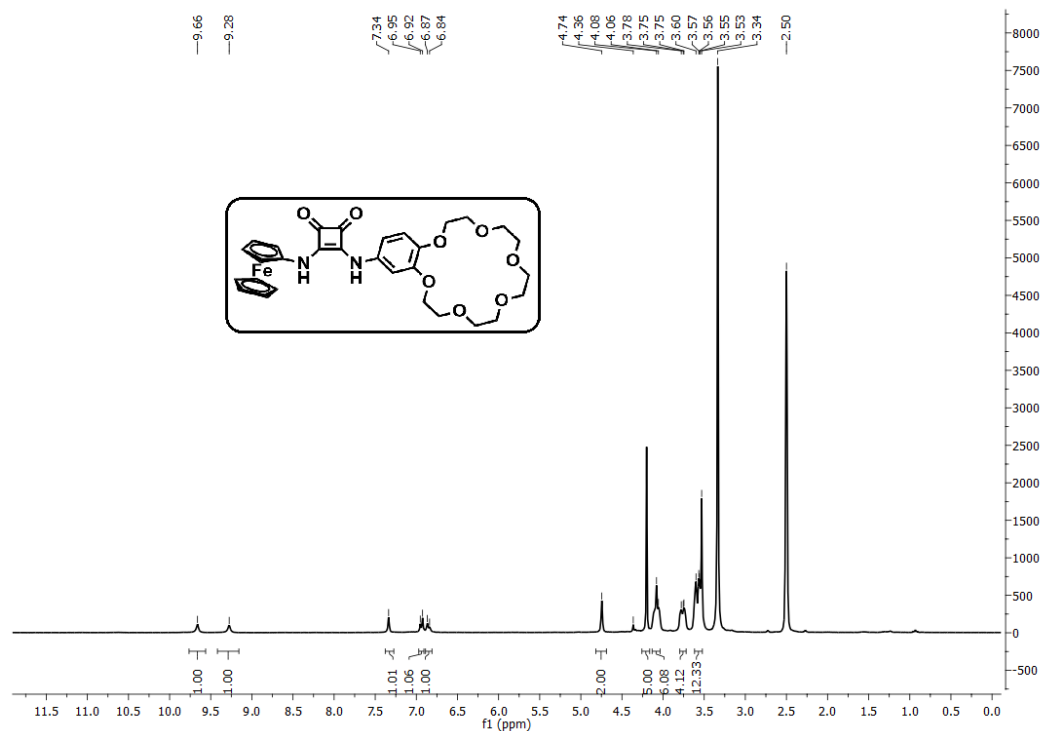


Fig. S9: ^1H NMR spectrum of receptor **2** in DMSO.

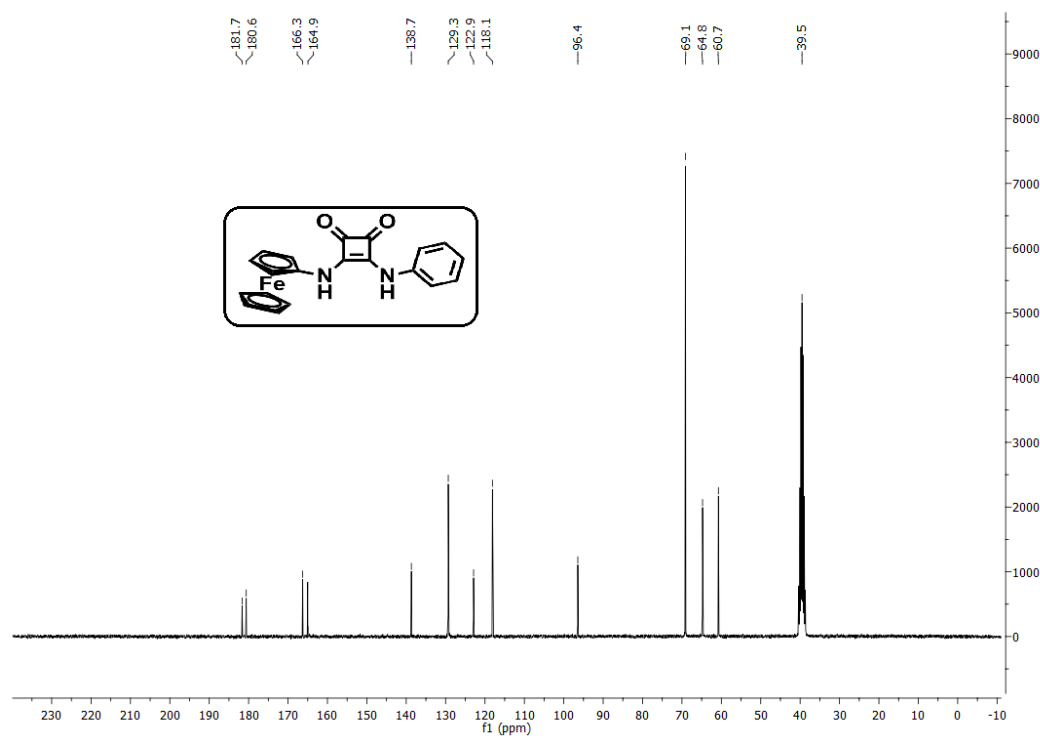


Fig. S12: ^{13}C NMR spectrum of receptor **3** in DMSO.

2. UV-vis titration experiments

UV-Vis experiment general procedure. UV-Vis titration experiments were performed on a Thermo Spectronic Unicam UV 500 spectrophotometer in CH_3CN solution at 298K. To 10 mm cuvette was added 2.5 mL of freshly prepared 2.6×10^{-5} M solution of studied receptor and in case of salts binding studies 1 mol equivalent of cation (KPF_6 or NaClO_4). Small aliquots of $\sim 2.0 \times 10^{-3}$ M TBAX solution containing receptor 1, receptor 2 or receptor 3 at the same concentration as in cuvette, were added and a spectrum was acquired after each addition. The resulting titration data were analyzed using BindFit (v0.5) package, available online at <http://supramolecular.org>. The stoichiometry determination was done using continuous variation method (Job plot).

2.1. Dilution plots.

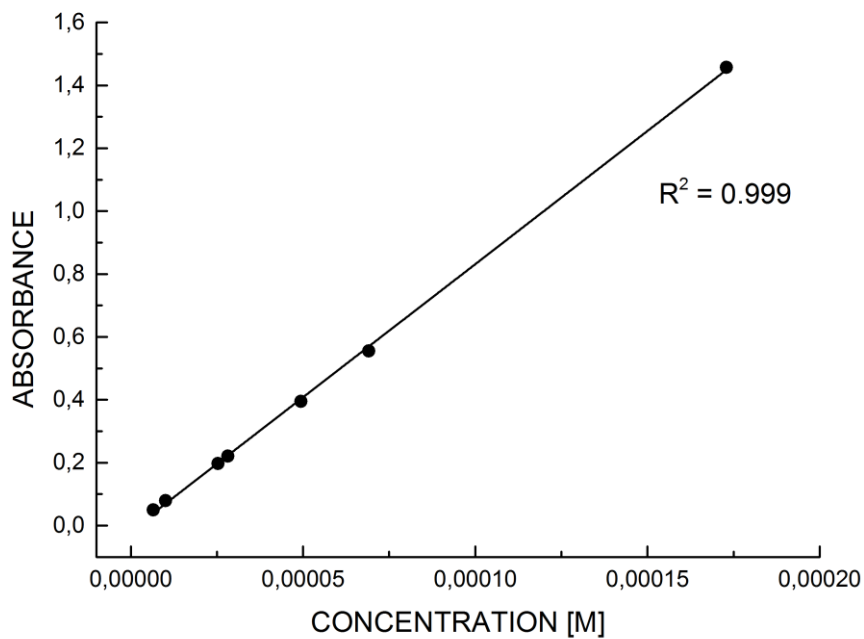


Fig. S13: Dilution curve of receptor 1.

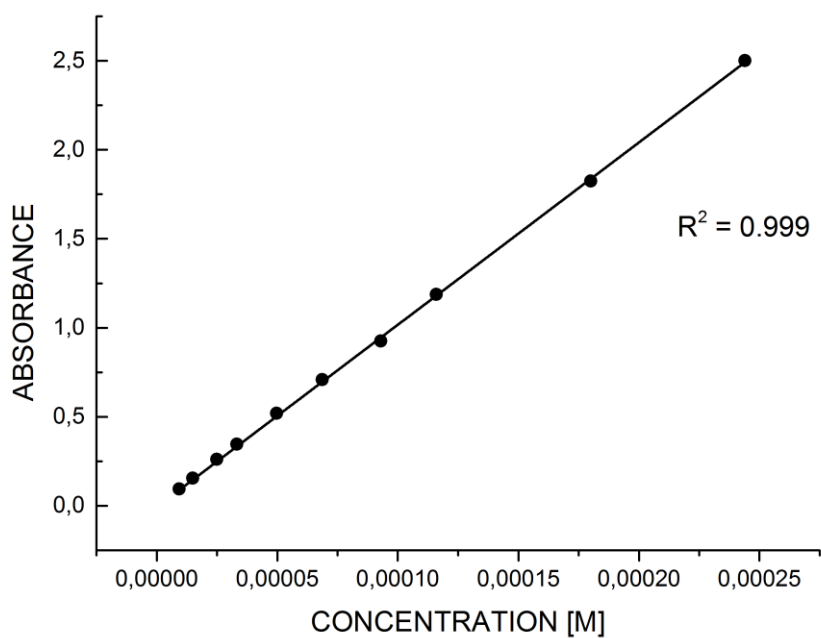


Fig. S14: Dilution curve of receptor 2.

2.2. Job plots:

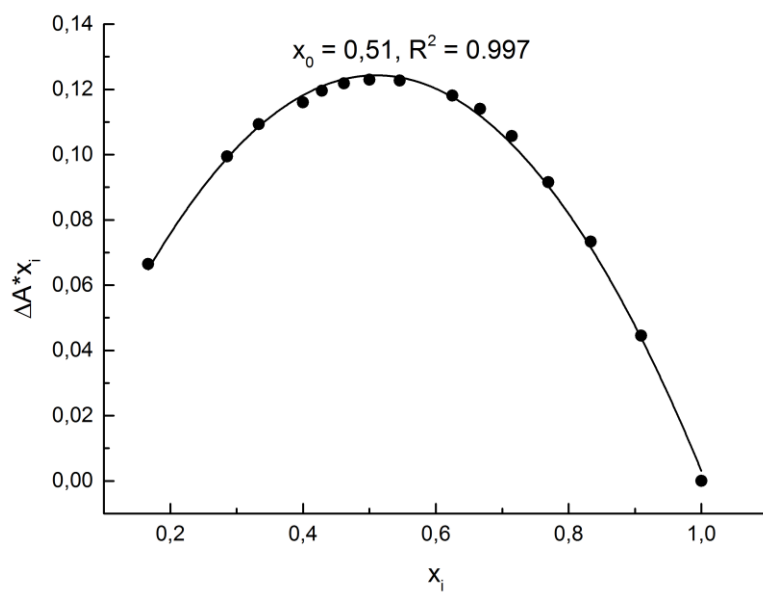


Fig. S15: Job plot analysis for **1** + TBACl.

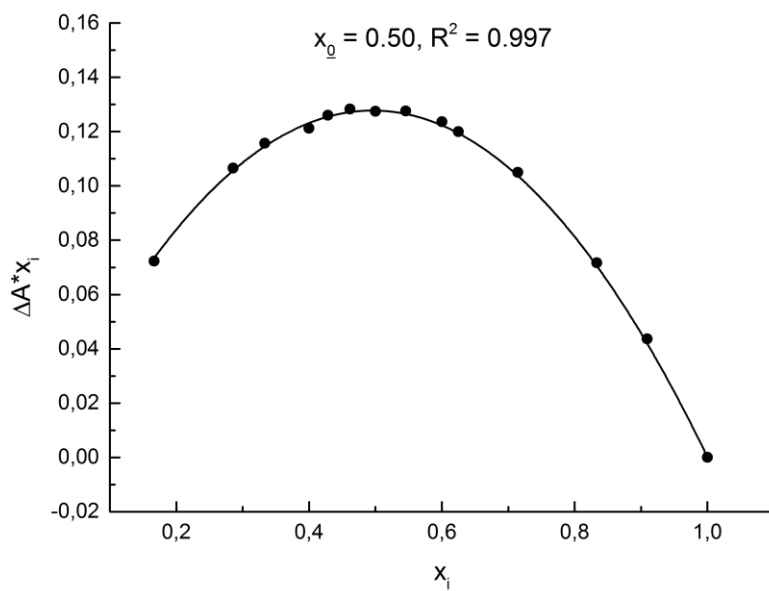


Fig. S16: Job plot analysis for **1** + NaClO₄.

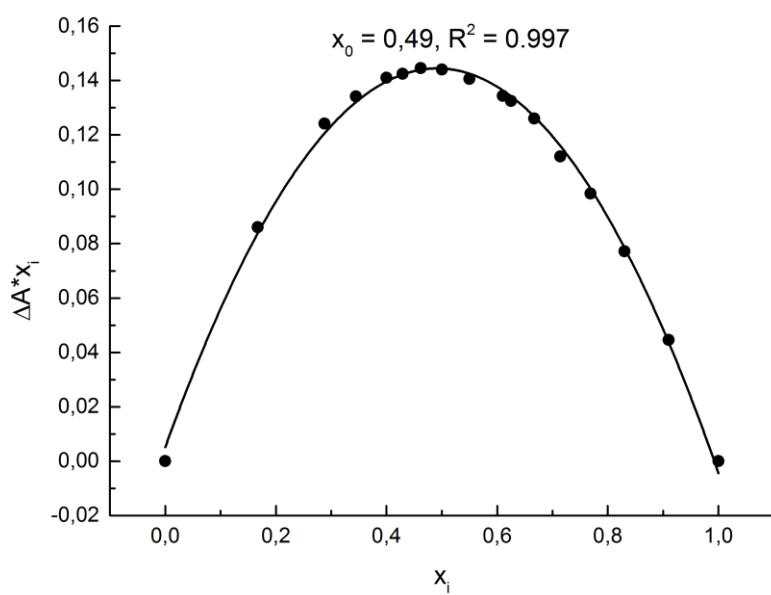


Fig. S17: Job plot analysis for **2** + KPF₆.

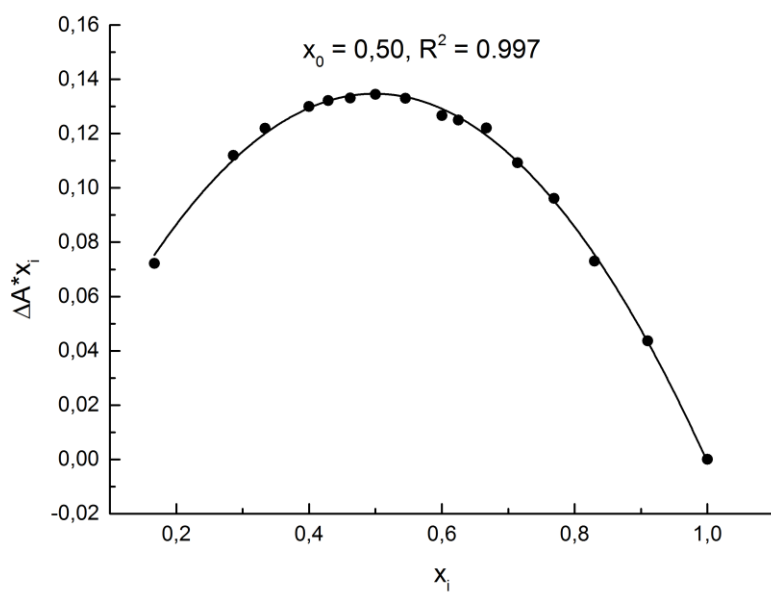


Fig. S18: Job plot analysis for **2** + TBACl.

2.3. Binding isotherms

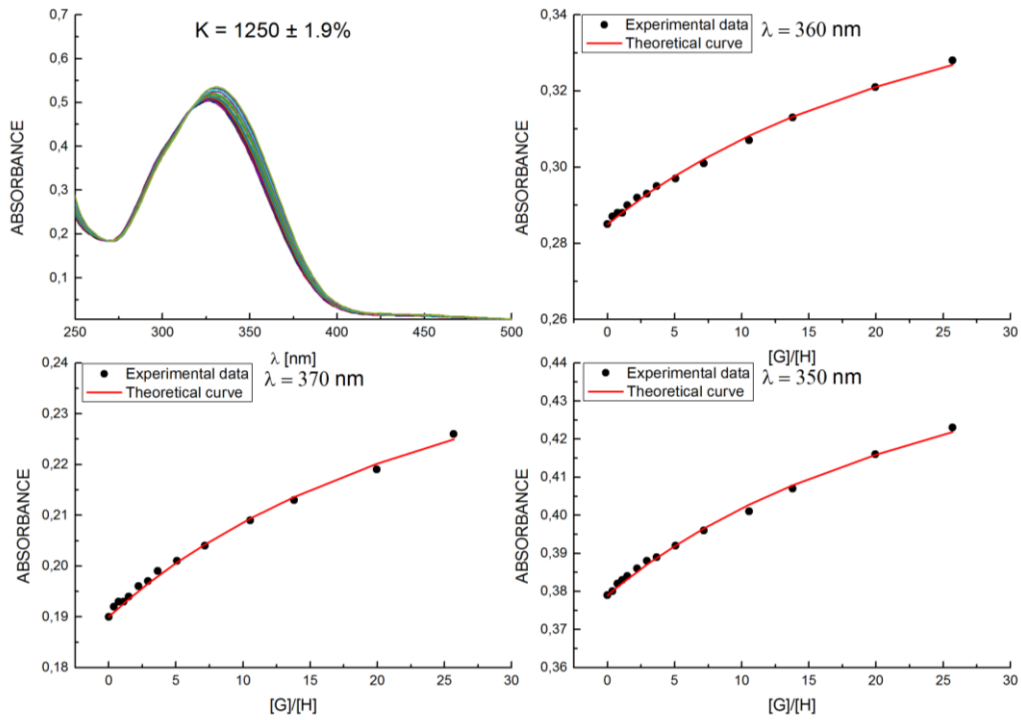


Fig. S19: UV-Vis titration of receptor 1 with TBANO₃ and selected binding isotherms.

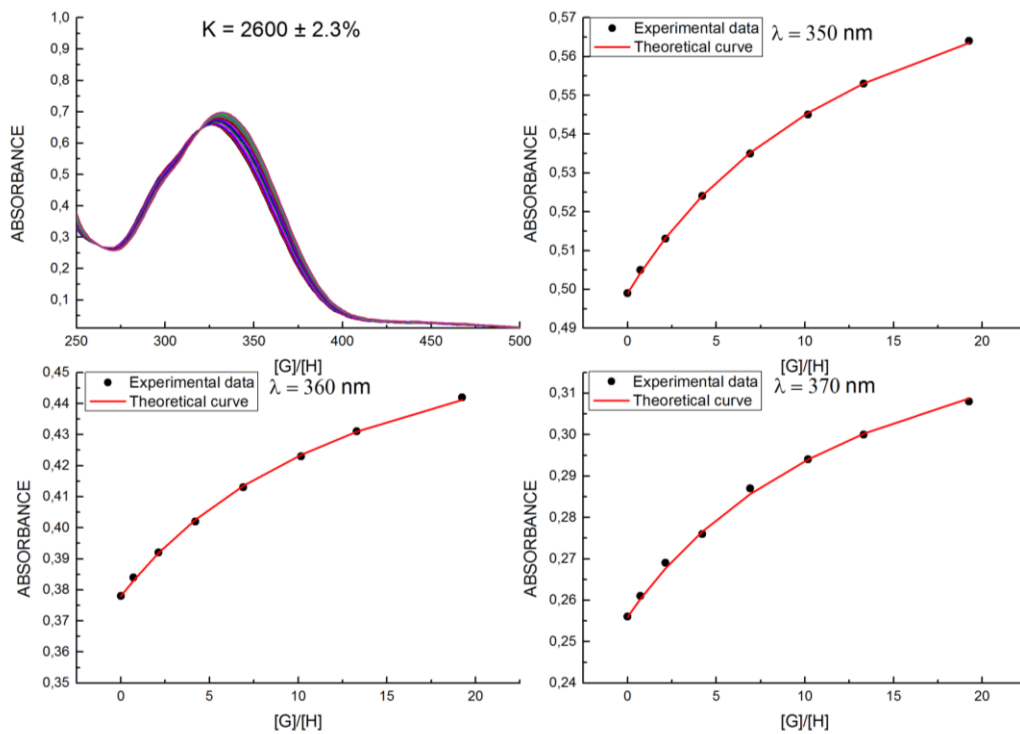


Fig. S20: UV-Vis titration of receptor 1 with TBANO₃ in the presence of 1 equivalent of NaClO₄ and selected binding isotherms.

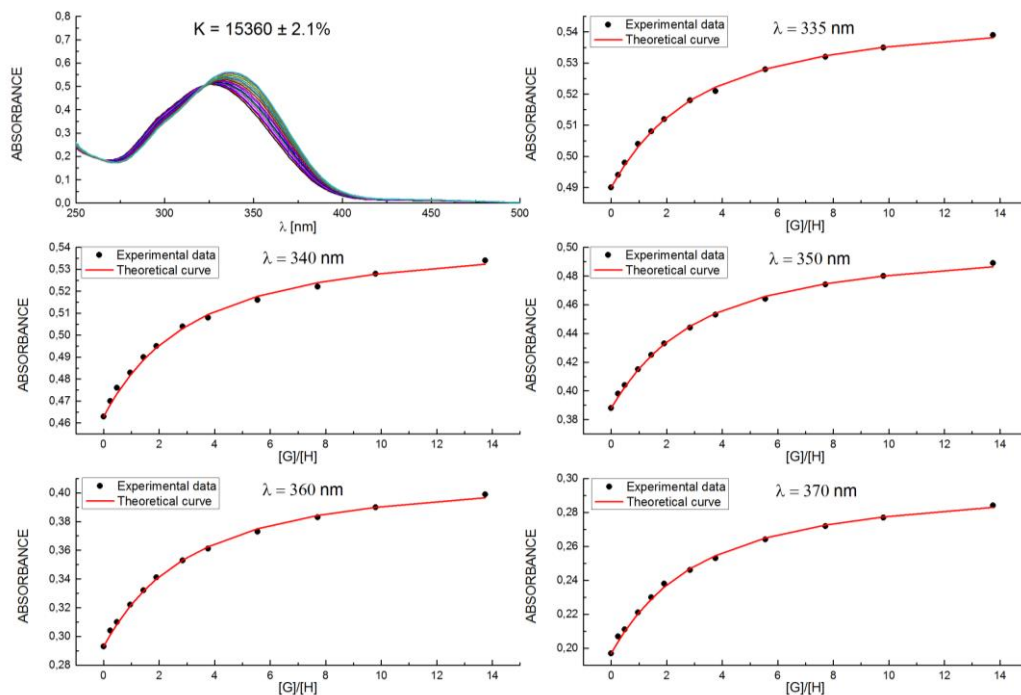


Fig. S21: UV-Vis titration of receptor 1 with TBABr and selected λ binding isotherms.

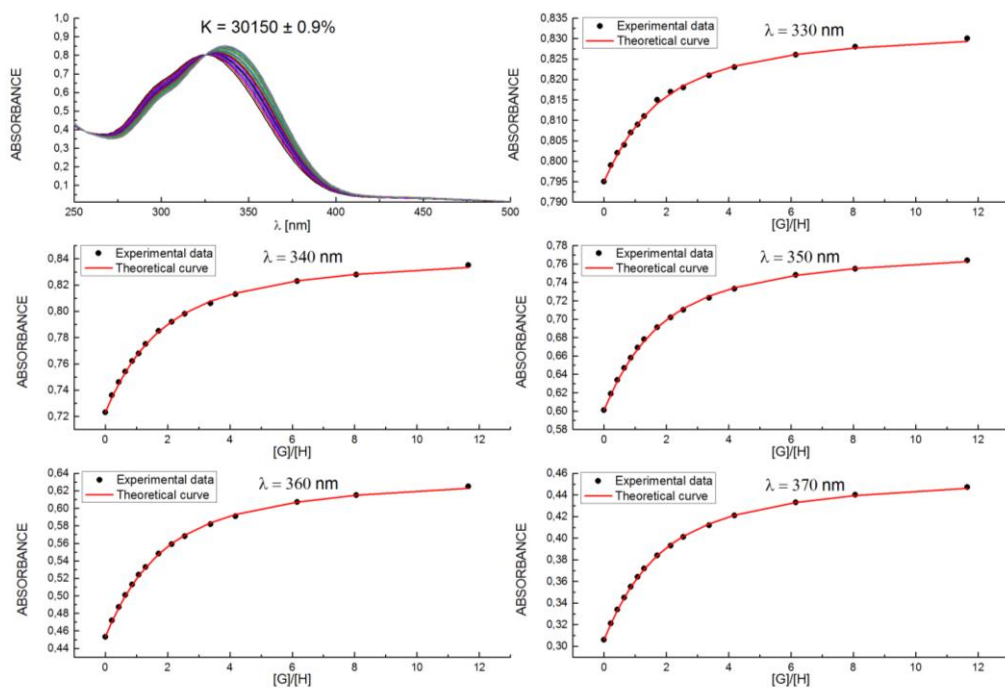


Fig. S22: UV-Vis titration of receptor 1 with TBABr in the presence of 1 equivalent of NaClO_4 and selected binding isotherms.

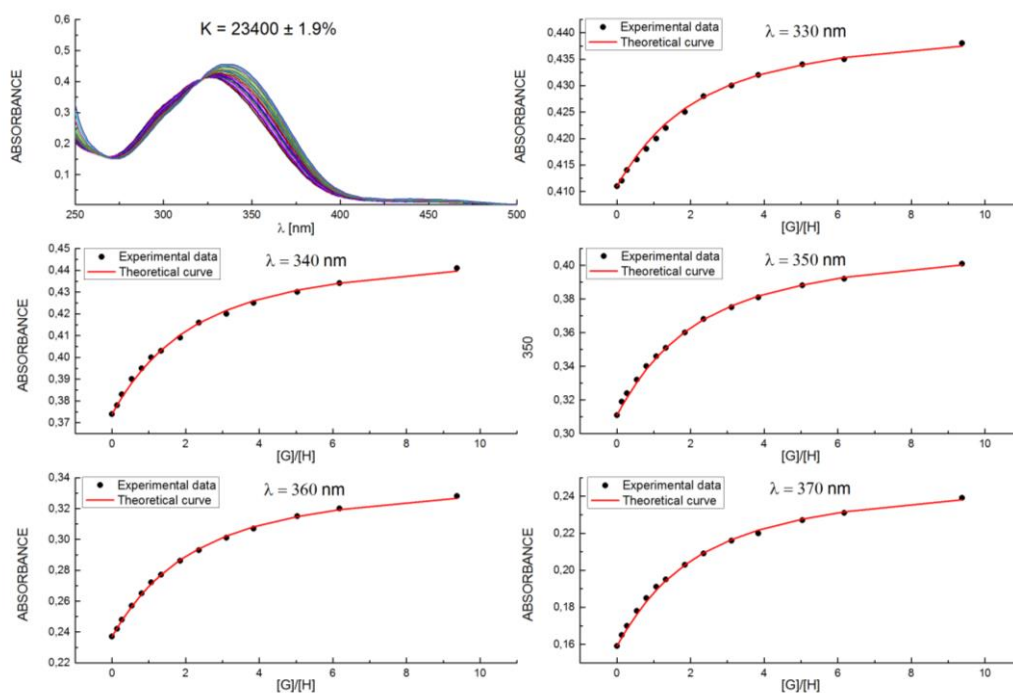


Fig. S23: UV-Vis titration of receptor **1** with TBANO₂ and selected binding isotherms.

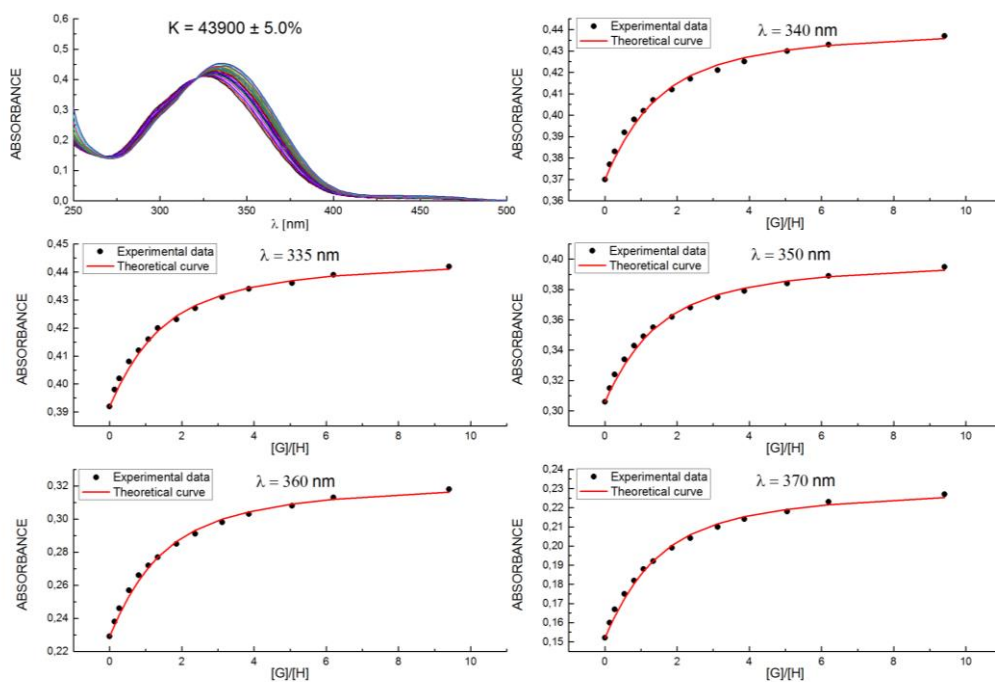


Fig. S24: UV-Vis titration of receptor **1** with TBANO₂ in the presence of 1 equivalent of NaClO₄ and selected binding isotherms.

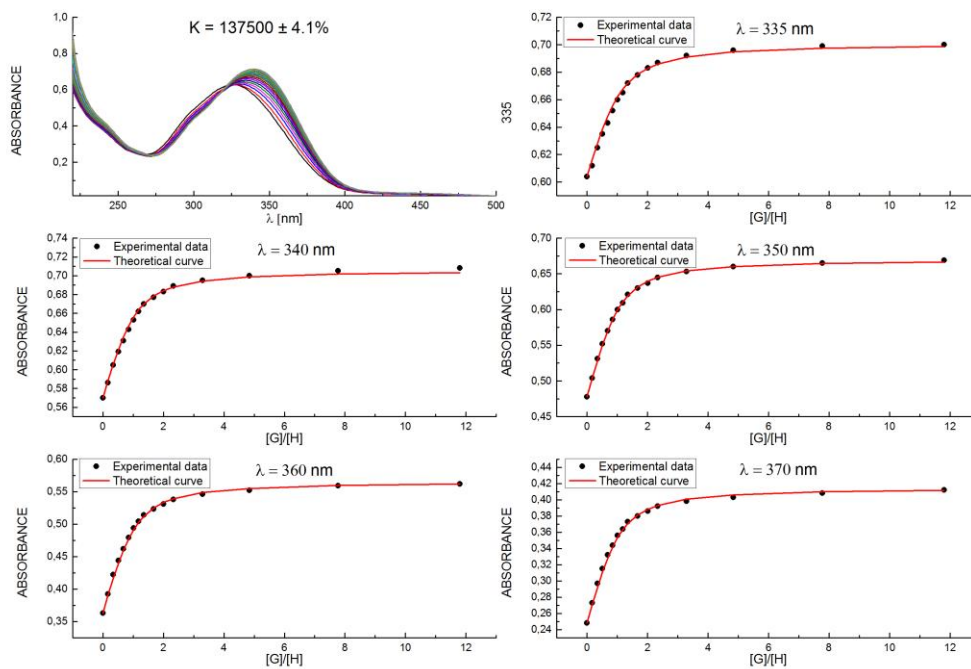


Fig. S25: UV-Vis titration of receptor **1** with TBACl and selected binding isotherms.

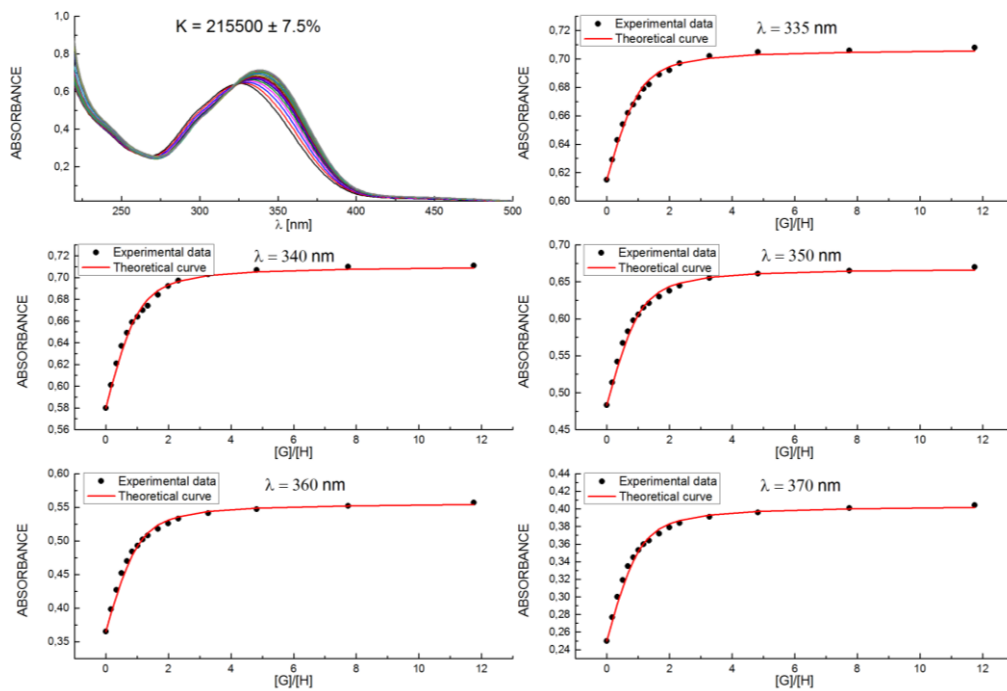


Fig. S26: UV-Vis titration of receptor **1** with TBACl in the presence of 1 equivalent of NaClO_4 and selected binding isotherms.

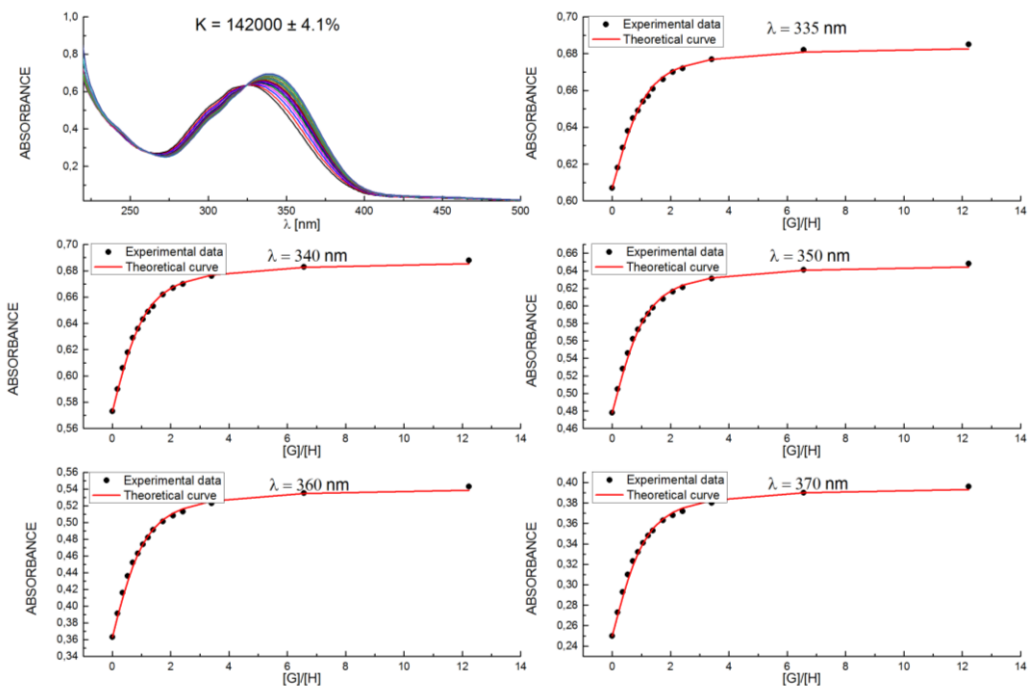


Fig. S27: UV-Vis titration of receptor 1 with TBACl in the presence of 1 equivalent of KPF₆ and selected binding isotherms.

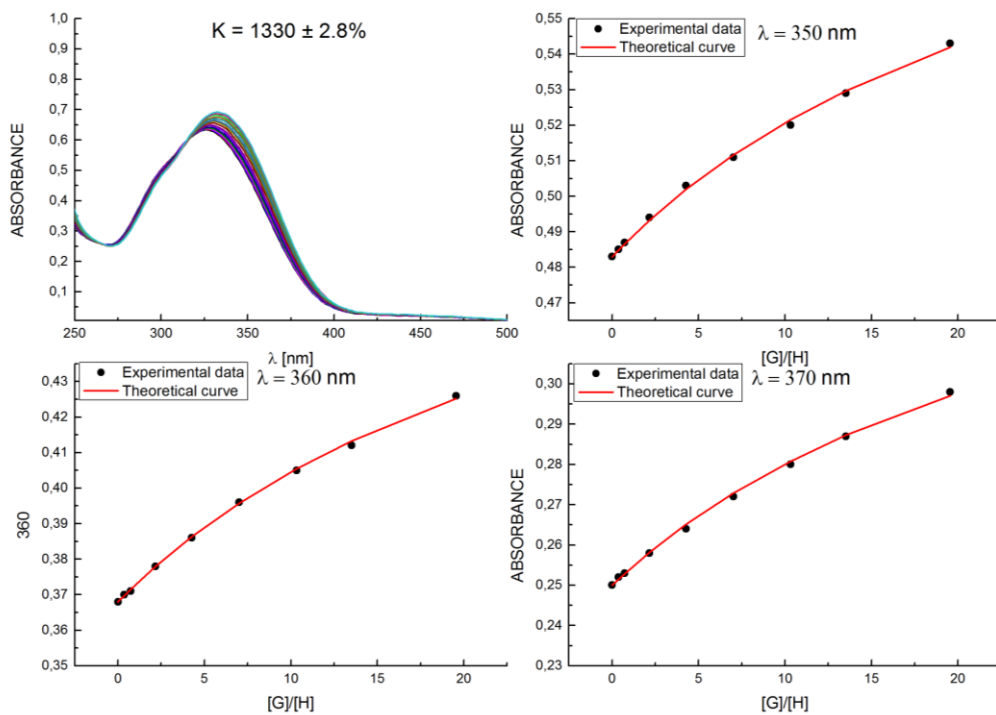


Fig. S28: UV-Vis titration of receptor 2 with TBANO₃ and selected binding isotherms.

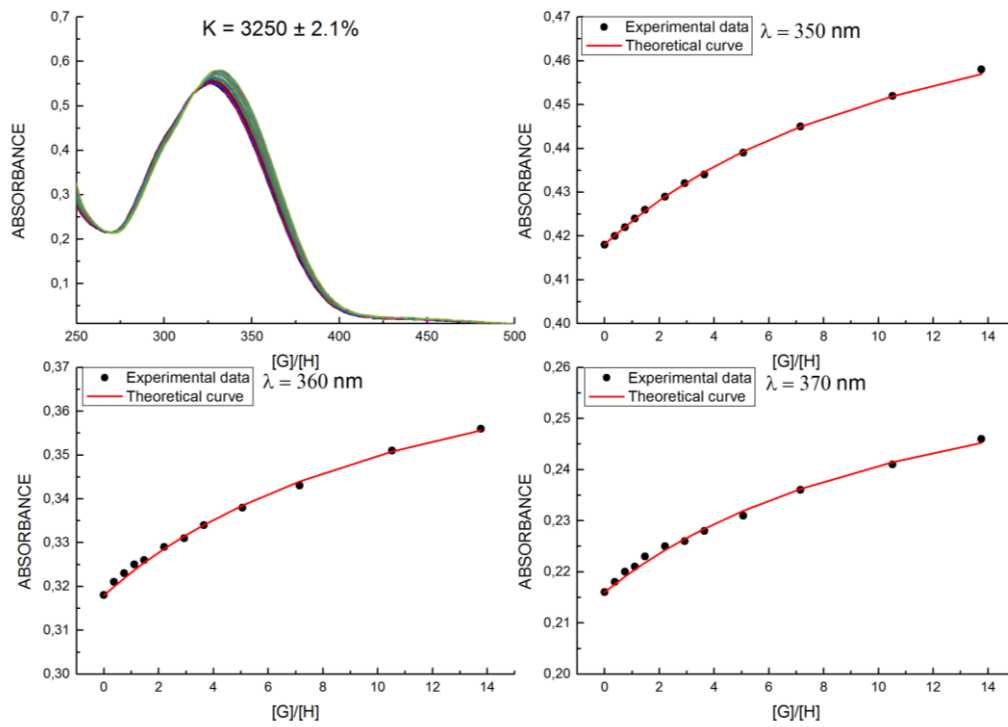


Fig. S29: UV-Vis titration of receptor **2** with TBANO₃ in the presence of 1 equivalent of NaClO₄ and selected binding isotherms.

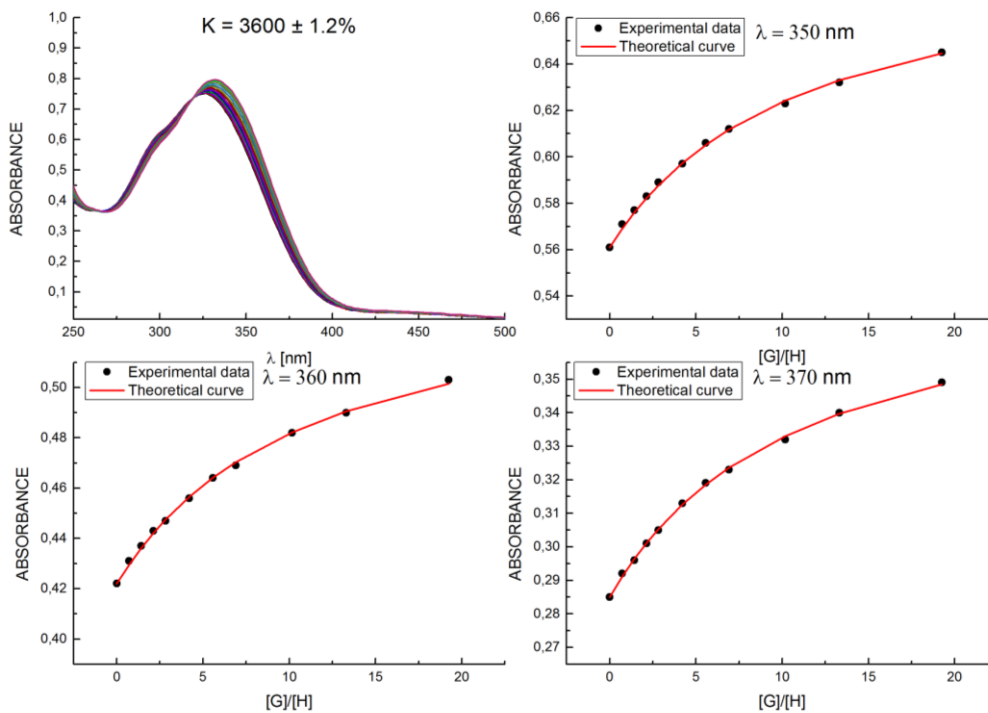


Fig. S30: UV-Vis titration of receptor **2** with TBANO₃ in the presence of 1 equivalent of KPF₆ and selected binding isotherms.

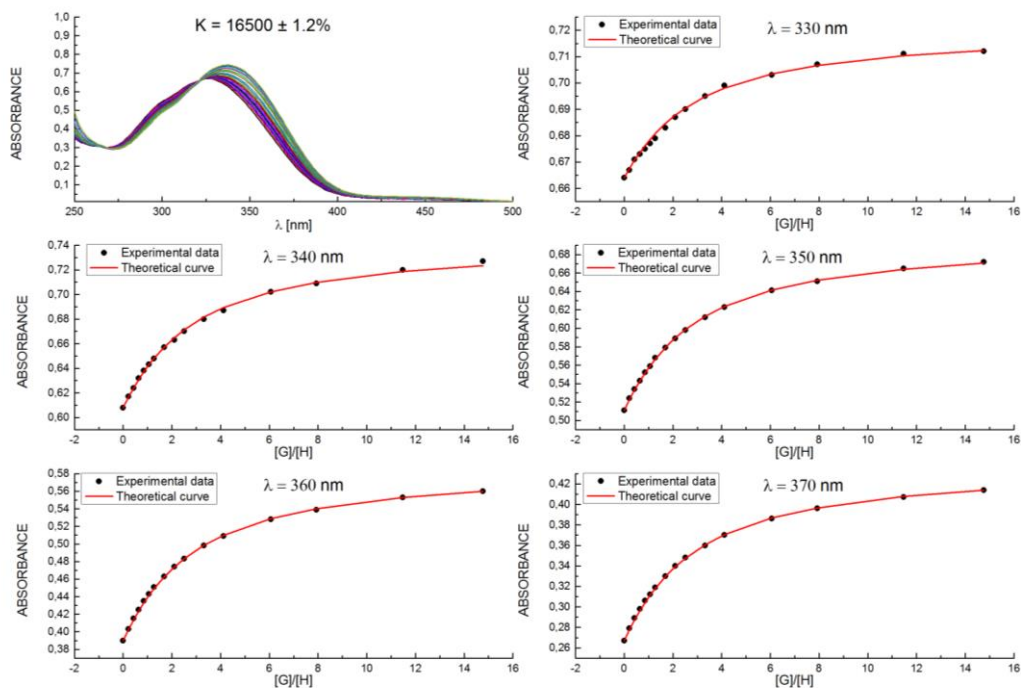


Fig. S31: UV-Vis titration of receptor **2** with TBABr and selected binding isotherms.

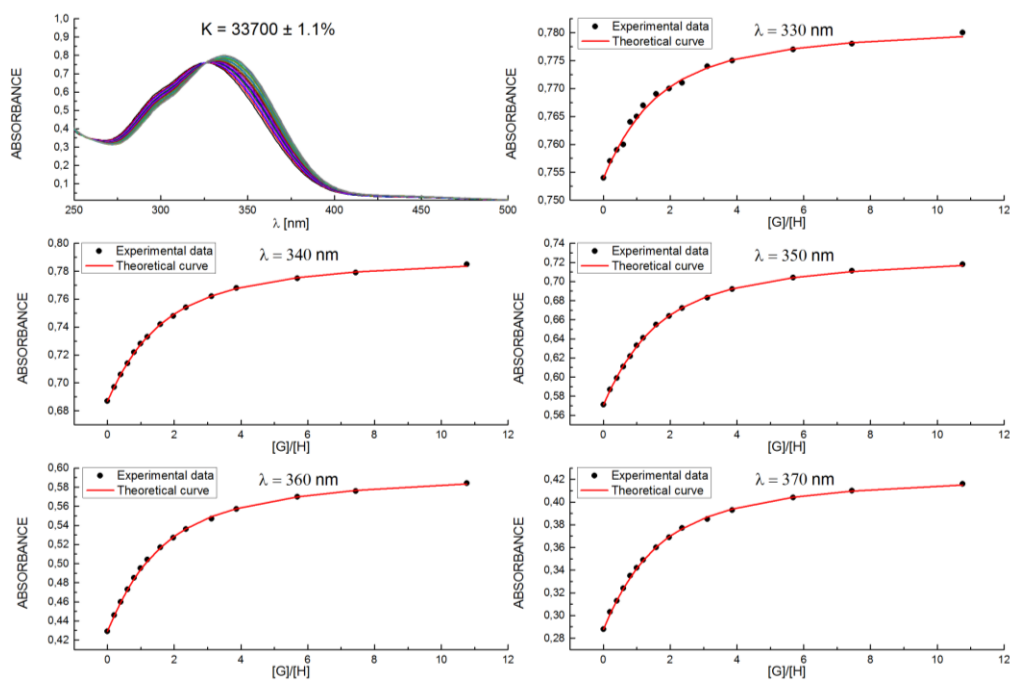


Fig. S32: UV-Vis titration of receptor **2** with TBABr in the presence of 1 equivalent of NaClO_4 and selected binding isotherms.

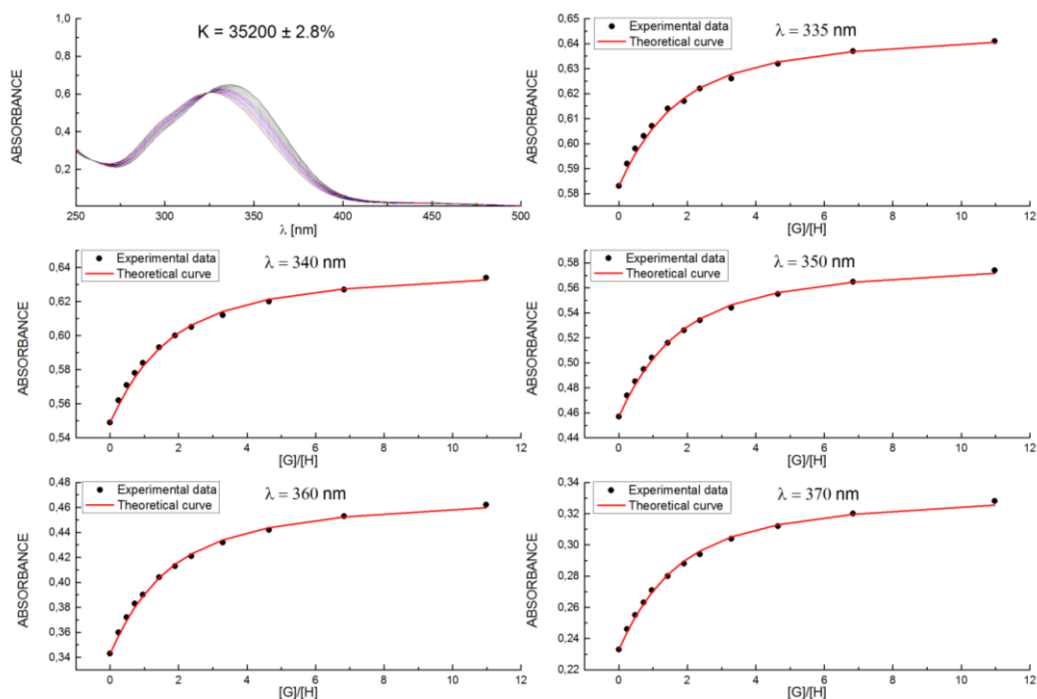


Fig. S33: UV-Vis titration of receptor 2 with TBABr in the presence of 1 equivalent of KPF₆ and selected binding isotherms.

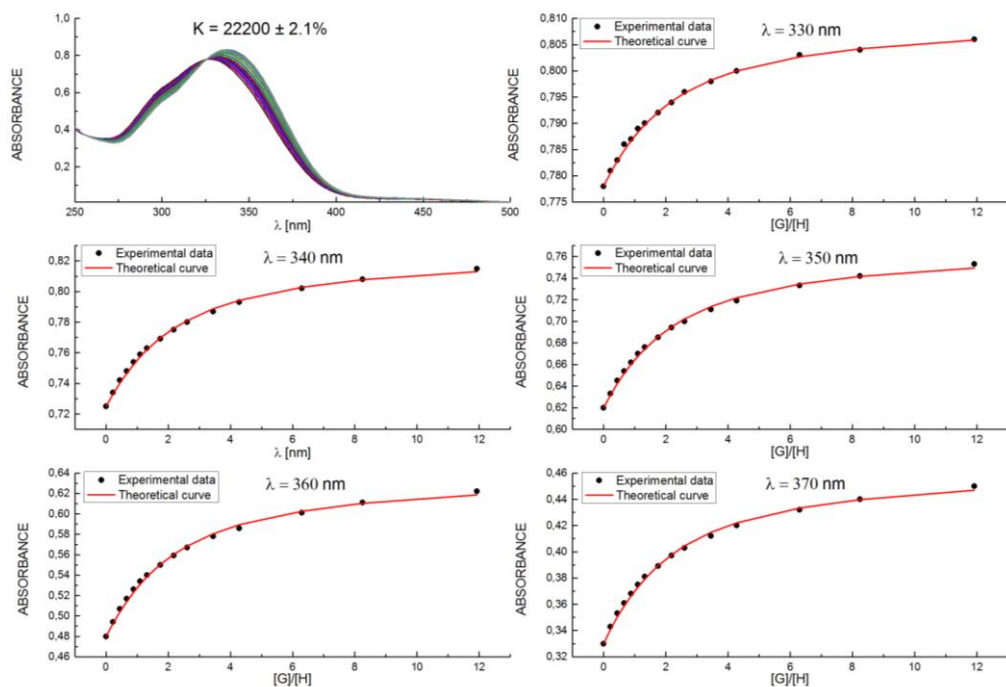


Fig. S34: UV-Vis titration of receptor 2 with TBANO₂ and selected binding isotherms.

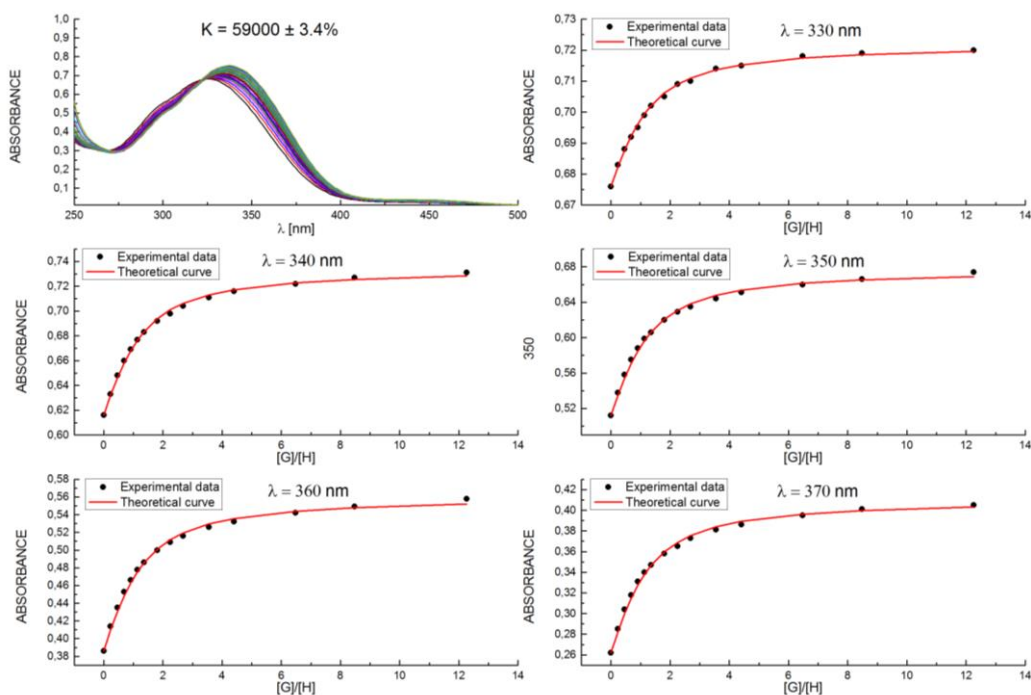


Fig. S35: UV-Vis titration of receptor **2** with TBANO₂ in the presence of 1 equivalent of NaClO₄ and selected binding isotherms.

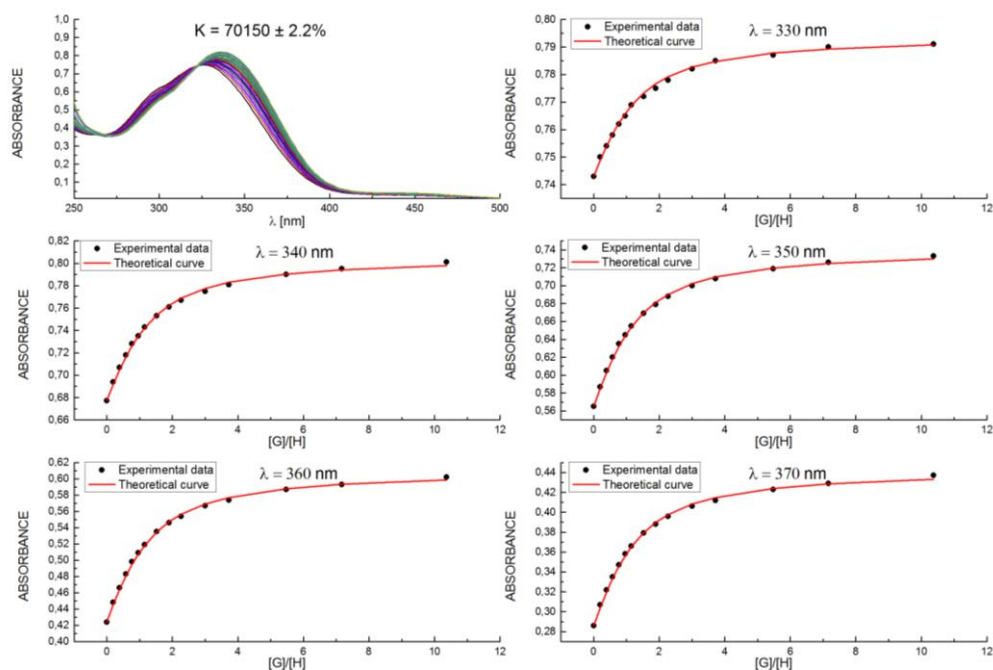


Fig. S36: UV-Vis titration of receptor **2** with TBANO₂ in the presence of 1 equivalent of KPF₆ and selected binding isotherms.

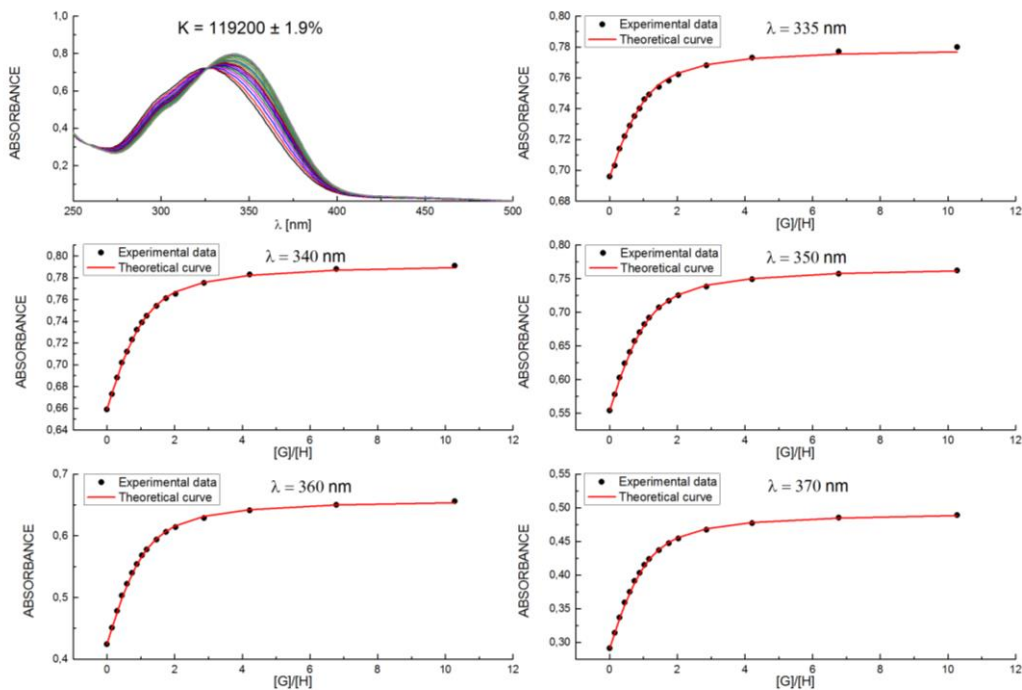


Fig. S37: UV-Vis titration of receptor **2** with TBACl and selected binding isotherms.

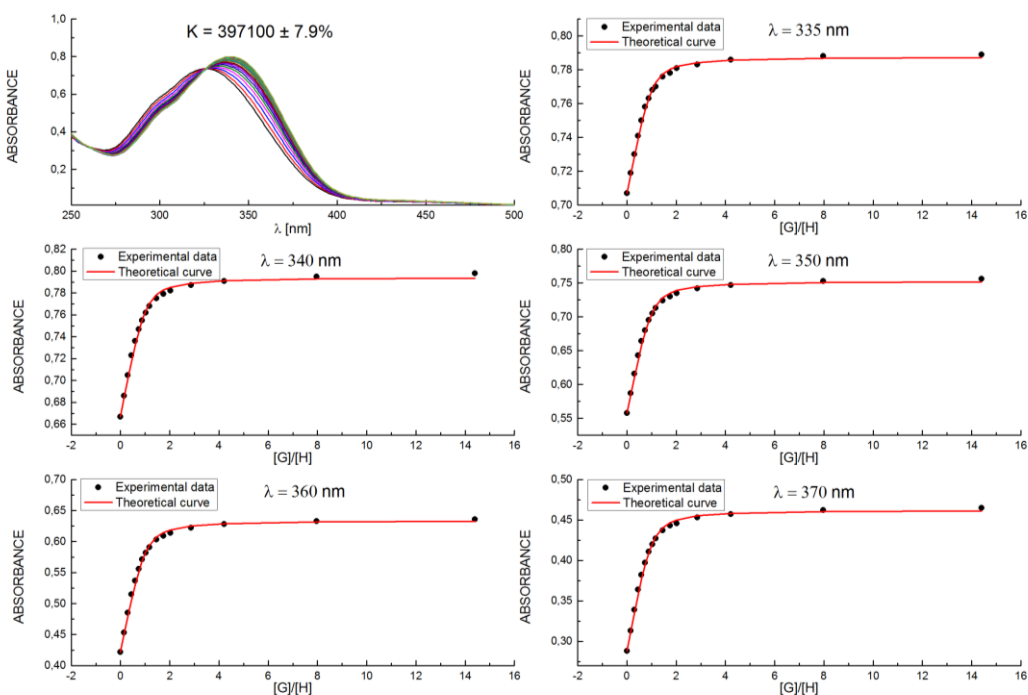


Fig. S38: UV-Vis titration of receptor **2** with TBACl in the presence of 1 equivalent of NaClO_4 and selected binding isotherms.

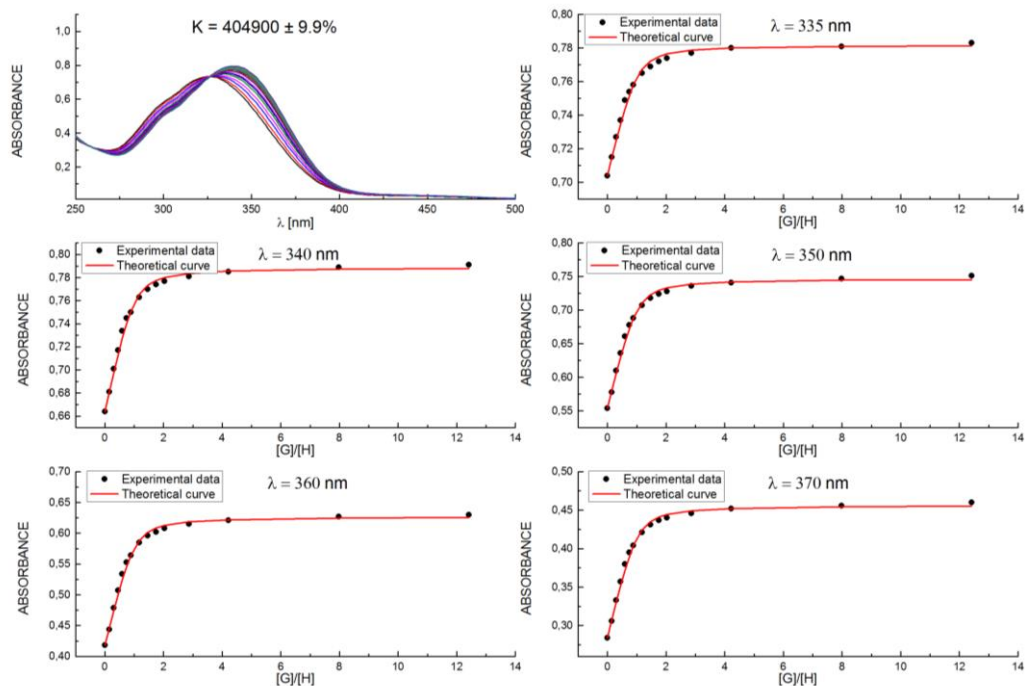


Fig. S39: UV-Vis titration of receptor **2** with TBACl in the presence of 1 equivalent of KPF_6 and selected binding isotherms.

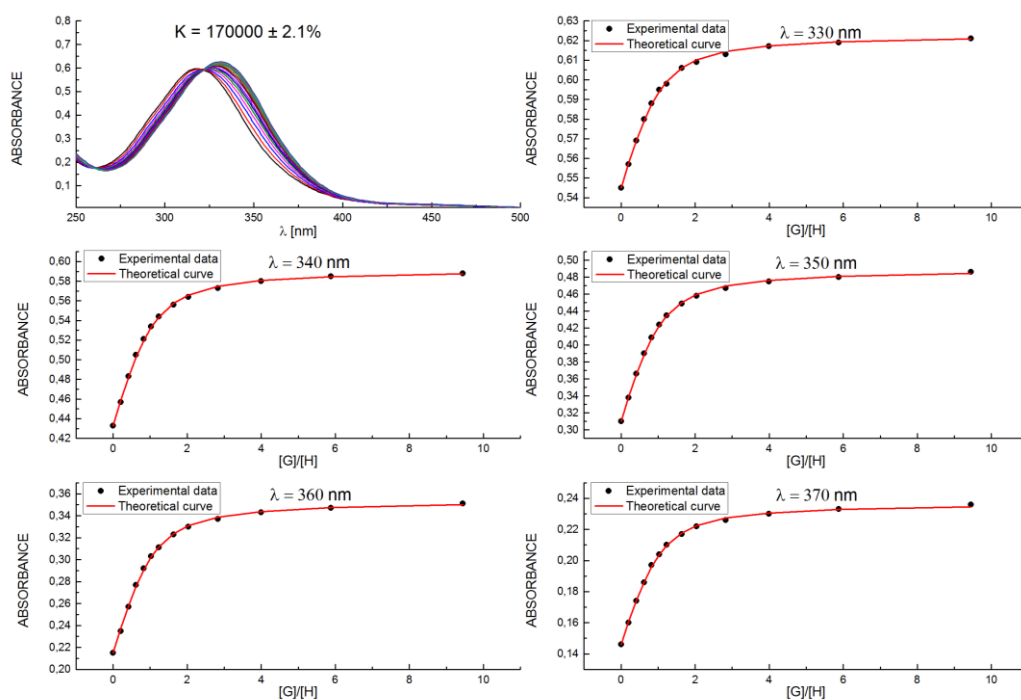


Fig. S40: UV-Vis titration of receptor **3** with TBACl and selected binding isotherms.

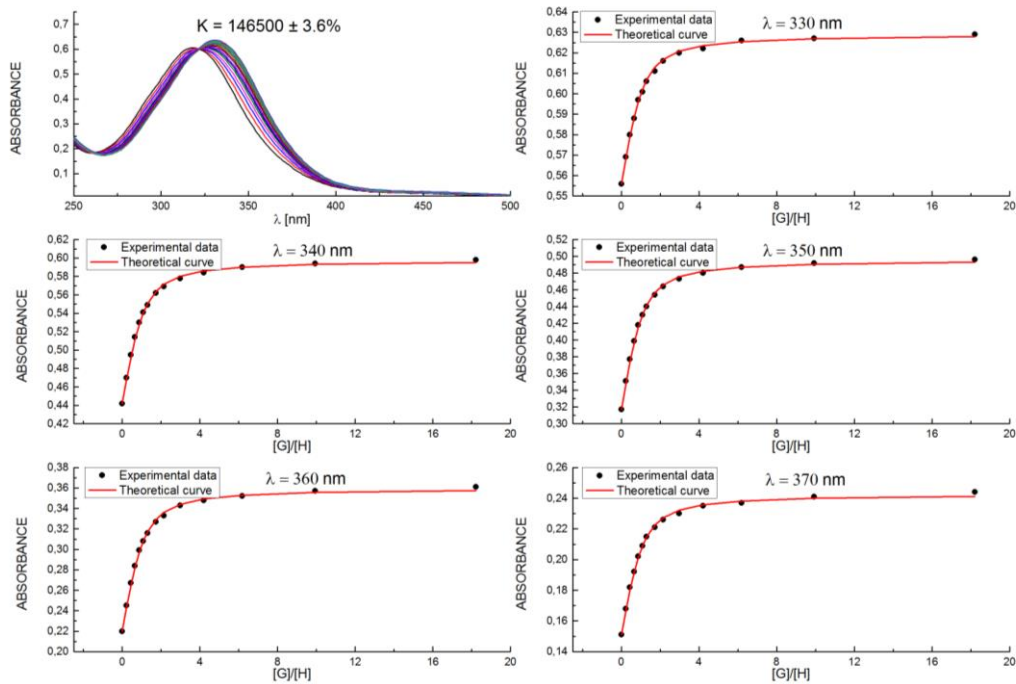


Fig. S41: UV-Vis titration of receptor **3** with TBACl in the presence of 1 equivalent of NaClO_4 and selected binding isotherms.

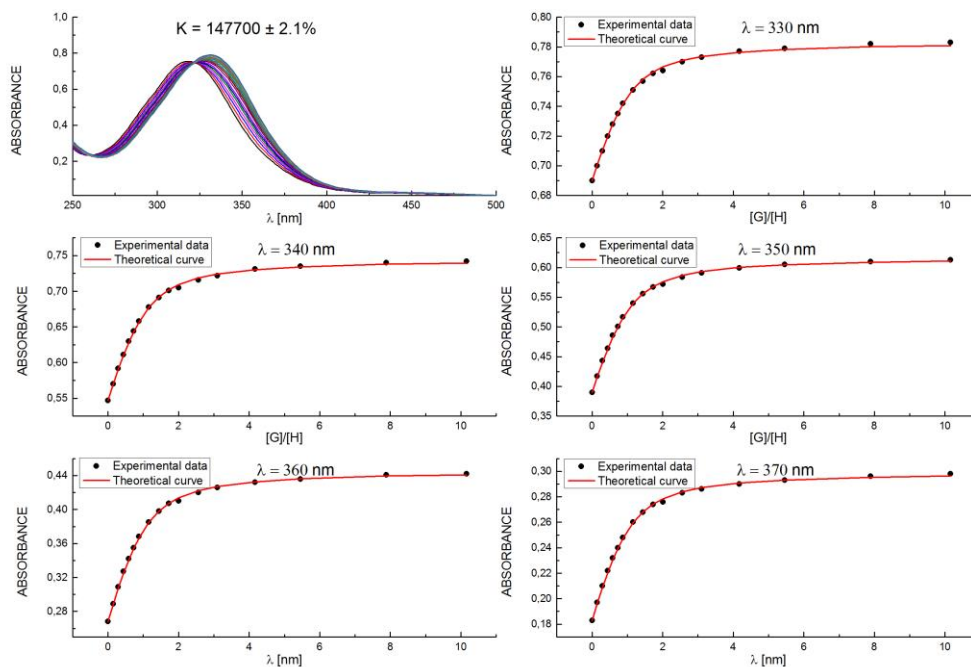


Fig. S42: UV-Vis titration of receptor **3** with TBACl in the presence of 1 equivalent of KPF_6 and selected binding isotherms.

3.NMR Titration

^1H NMR titration experiments were performed on a 300 MHz BrukerAvance spectrometer, at 298K, in CD_3CN solution. In each case 0.5 mL of 1.1×10^{-3} solution of receptor 1 or receptor 2 was added to 5 mm NMR tube. In the case of ion pair titration receptor was firstly pretreated with one equivalent of NaClO_4 or KPF_6 . Then small aliquots of solution of TBAX, containing receptor 1 or receptor 2 at constant concentration, were added and a spectrum was acquired after each addition. The resulting titration data were analyzed using BindFit (v0.5) package, available online at <http://supramolecular.org>.

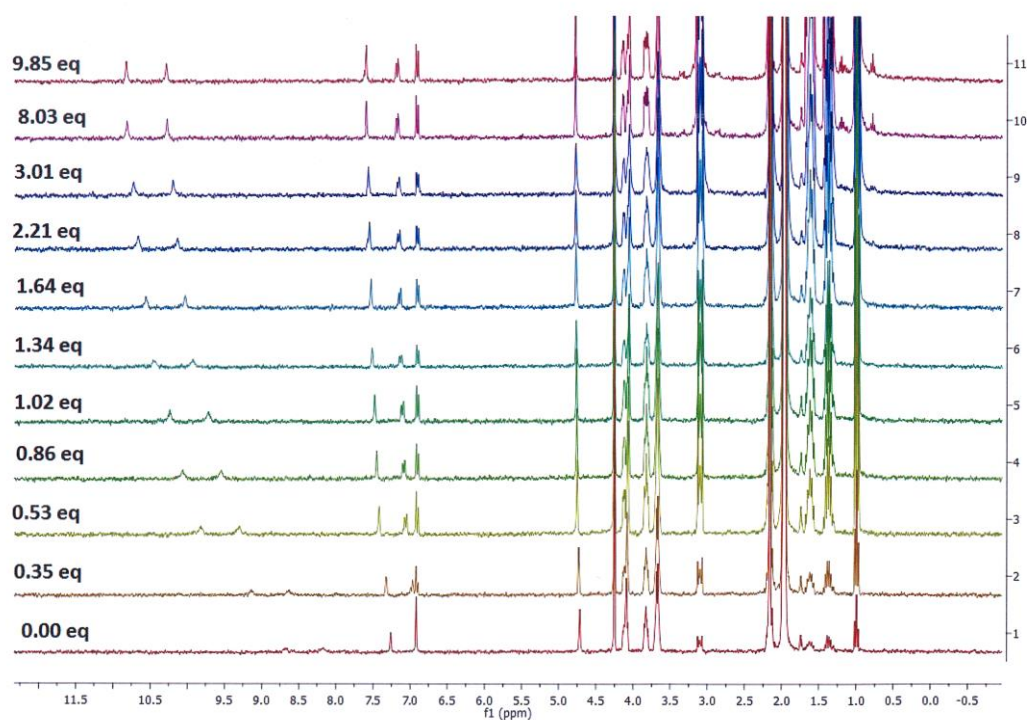


Fig. S43: Variation of the ^1H NMR spectrum recorded upon titration of receptor 1 in CD_3CN with TBABr.

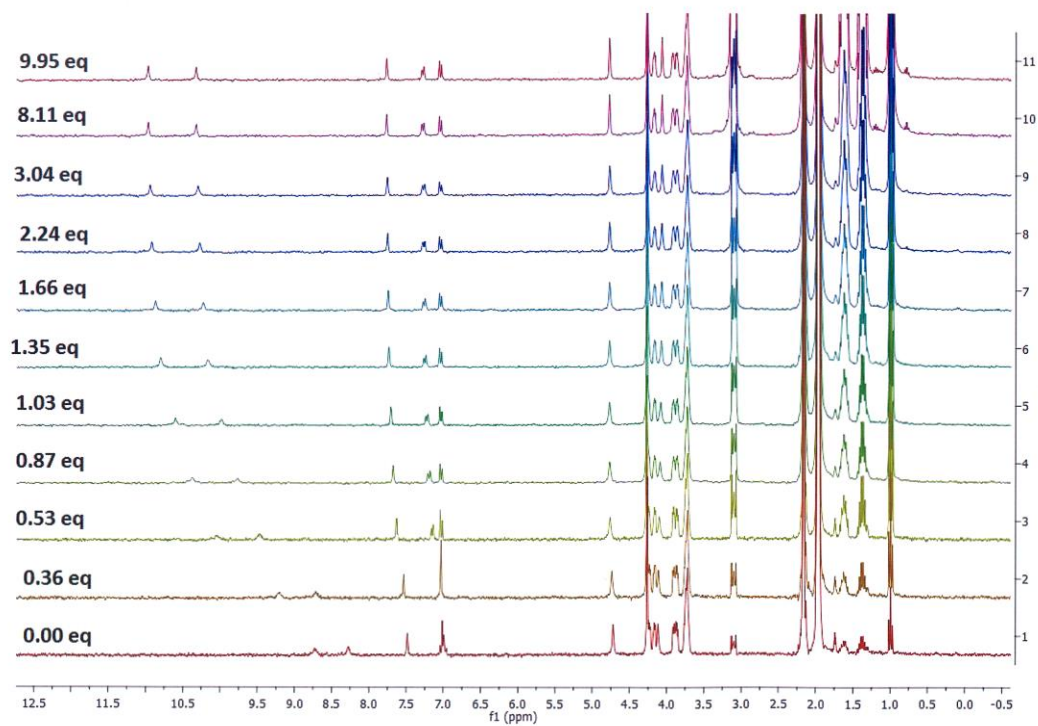


Fig. S44: Variation of the ^1H NMR spectrum recorded upon titration of receptor **1** in CD_3CN with TBABr in the presence of 1 eq. NaClO_4 .

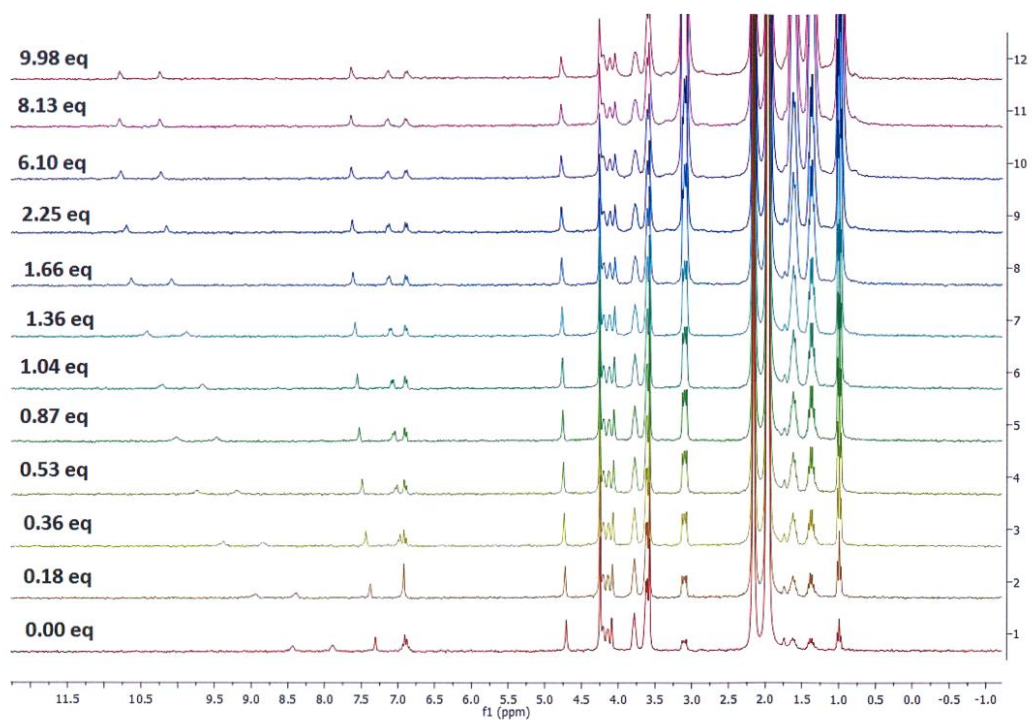


Fig. S45: Variation of the ^1H NMR spectrum recorded upon titration of receptor **2** in CD_3CN with TBABr.

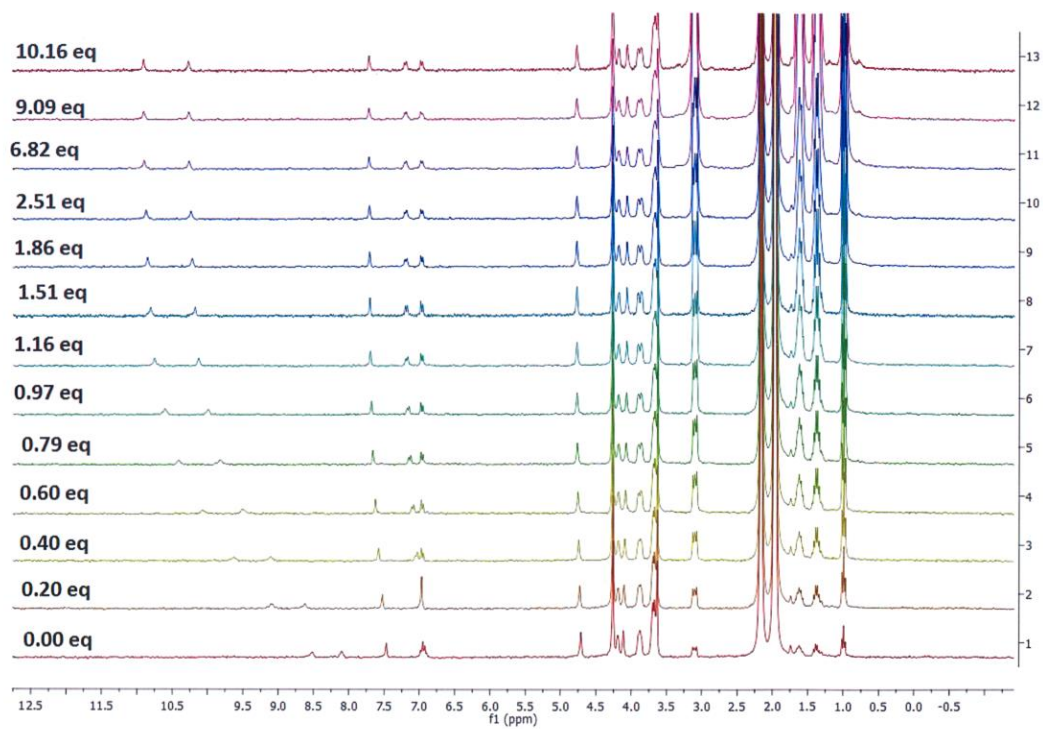


Fig. S46: Variation of the ^1H NMR spectrum recorded upon titration of receptor **2** in CD_3CN with TBABr in the presence of 1 eq. KPF_6 .

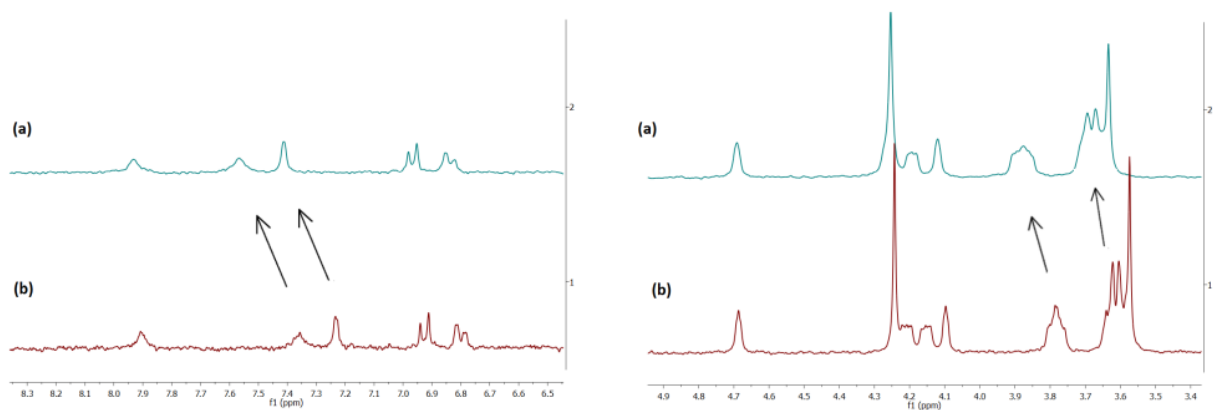


Fig. S47: Partial ^1H NMR spectra (from left: aromatic and squaramide region ; from right: crown ether region) of (a) receptor **2** in the presence of 1 eq. KPF_6 (b) receptor **2** in CD_3CN .

4. Electrochemical measurements

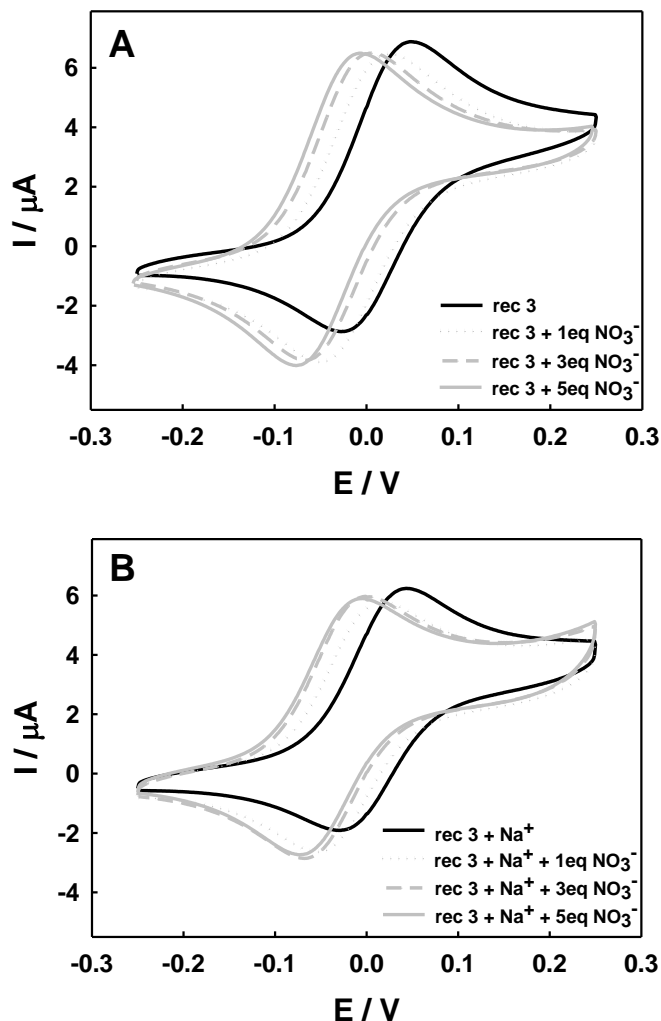


Fig. S48: Cyclic voltammograms recorded for 0.5 mM solution of receptor 3 (solid black line), after adding 1, 3, and 5 equiv. of TBANO₃ (gray lines) (A); after adding 1 equiv. of NaClO₄ (dashed black line) and then after adding 1, 3, and 5 equiv. of TBANO₃ (gray lines) (B) in acetonitrile. The concentration of supporting electrolyte TBAPF₆ was 0.1 M, and scan rate was 100 mV s⁻¹.

5. X-Ray crystallographic data

Single crystal X-Ray diffraction 1-NaCl. The X-ray measurement of **1-NaCl** was performed at 200(2) K on a Bruker D8 Venture Photon100 diffractometer equipped with a TRIUMPH monochromator and a MoK α fine focus sealed tube ($\lambda = 0.71073 \text{ \AA}$). A total of 1160 frames were collected with Bruker APEX2 program [1]. The frames were integrated with the Bruker SAINT software package [2] using a narrow-frame algorithm. The integration of the data using a tetragonal unit cell yielded a total of 82454 reflections to a maximum ϑ angle of 25.05° (0.84 \AA resolution), of which 6101 were independent (average redundancy 13.515, completeness = 99.9%, $R_{int} = 5.40\%$, $R_{sig} = 2.85\%$) and 3951

(64.76%) were greater than $2\sigma(F^2)$. The final cell constants of $a = 24.353(2) \text{ \AA}$, $c = 23.276(2) \text{ \AA}$, $V = 13804.(3) \text{ \AA}^3$, are based upon the refinement of the XYZ-centroids of 9882 reflections above $20 \sigma(I)$ with $4.731^\circ < 2\theta < 45.33^\circ$. Data were corrected for absorption effects using the multi-scan method (SADABS) [3]. The ratio of minimum to maximum apparent transmission was 0.913. The calculated minimum and maximum transmission coefficients (based on crystal size) are 0.855 and 0.934.

The structure was solved and refined using SHELXTL Software Package [4,5] using the space group $I4_1/a$, with $Z = 16$ for the formula unit, $C_{28.75}H_{30}ClFeN_2NaO_7$. The final anisotropic full-matrix least-squares refinement on F^2 with 436 variables converged at $R1 = 6.64\%$, for the observed data and $wR2 = 24.25\%$ for all data. The goodness-of-fit was 1.138. The largest peak in the final difference electron density synthesis was $0.573 \text{ e}^-/\text{\AA}^3$ and the largest hole was $-0.318 \text{ e}^-/\text{\AA}^3$ with an RMS deviation of $0.102 \text{ e}^-/\text{\AA}^3$. On the basis of the final model, the calculated density was 1.212 g/cm^3 and $F(000)$, 5224 e^- .

Structure is slightly disordered in the ferrocene fragment. Unsubstituted cyclopentadienyl (CP) anion is located in two alternative sites with refined occupancy of 0.50(2):0.50(2). There is additional position of Fe ion with occupancy of ca. 8% with not localized other CP units. This is due to relatively small residual electron density originating from C atoms all with low occupancy of 8%. In addition the structure contains unidentified disordered solvent molecules modeled by four carbon atoms with occupancies in the range from 0.25 to 0.15. The unit cell contains four voids of total volume equal to 380 \AA^3 (calculated in Mercury software [6]). These voids probably remains empty – the highest maximum electron density peak in the cell is less than $0.58 \text{ e}^-/\text{\AA}^3$. This is probably the reason why the crystals are damaged at temperatures below 200 K.

These unoccupied space is responsible for the structure collapse while the crystals are cooled below 200 K. Most of non-hydrogen atoms were refined anisotropically. The exception was made for ca. 8% occupancy disordered Fe ion and unidentified solvent molecule treated as not fully occupy carbon atoms. Most of hydrogen atoms were placed in calculated positions and refined within the riding model. Positions of two hydrogen atoms of urea fragment engaged in hydrogen bonds were refined together with their isotropic atomic displacement parameters. The temperature factors of other hydrogen atoms were not refined and were set to be equal to either 1.2 or 1.5 times larger than U_{eq} of the corresponding heavy atom. The atomic scattering factors were taken from the International Tables [7]. Molecular graphics was prepared using Mercury CSD 4.1.0 program [6]. Numbering scheme and thermal ellipsoids parameters are presented at 50% probability level in **Figure S49 a)**. Packing diagrams of **1-NaCl** crystal structure are shown in **Figure S49 a)**.

2-KCl. The X-ray measurement of **2-KCl** was performed at 100(2) K on a Bruker D8 Venture PhotonII diffractometer equipped with a TRIUMPH monochromator and a MoK α fine focus sealed tube ($\lambda = 0.71073$ Å). A total of 1690 frames were collected with Bruker APEX3 program [8]. The frames were integrated with the Bruker SAINT software package [9] using a narrow-frame algorithm. The integration of the data using a **monoclinic** unit cell yielded a total of **5755** reflections to a maximum ϑ angle of **25.04°** (**0.84** Å resolution), of which **5755** were independent (average redundancy **1.000**, completeness = **99.3%**, $R_{sig} = 4.76\%$) and **4575** (**79.50%**) were greater than $2\sigma(F^2)$. The final cell constants of $a = 37.465(2)$ Å, $b = 10.0612(5)$ Å, $c = 17.8868(9)$ Å, $\beta = 103.909(2)^\circ$, $V = 6544.6(6)$ Å³, are based upon the refinement of the XYZ-centroids of **9914** reflections above $20\sigma(I)$ with $4.480^\circ < 2\vartheta < 49.99^\circ$. Data were corrected for absorption effects using the multi-scan method (TWINABS) [10]. The ratio of minimum to maximum apparent transmission was **0.703**. The calculated minimum and maximum transmission coefficients (based on crystal size) are **0.852** and **0.969**.

The structure was solved and refined using SHELXTL Software Package [4,5] using the space group **C2/c**, with $Z = 4$ for the formula unit, **C₆₄H₇₈Cl₂Fe₂K₂N₄O₁₇**. The final anisotropic full-matrix least-squares refinement on F^2 with **464** variables converged at $R1 = 5.84\%$, for the observed data and $wR2 = 14.01\%$ for all data. The goodness-of-fit was **1.088**. The largest peak in the final difference electron density synthesis was **0.509** e⁻/Å³ and the largest hole was **-0.507** e⁻/Å³ with an RMS deviation of **0.079** e⁻/Å³. On the basis of the final model, the calculated density was **1.457** g/cm³ and $F(000)$, **3000** e⁻.

The measured sample was oligocrystalline containing a number of slightly rotated domains. Due to partial overlap of the diffraction spots integration of the reflections and scaling were based on four domains followed by the merging data to HKLF4 format with the refined twin fractions yielding: 0.3395, 0.3464, 0.0903, 0.2239.

In the structure aliphatic part of the crown ether fragment is disordered over two alternative positions with refined occupancy ratio of 0.609(9):0.391(9). In addition the structure contains disordered diethyl ether molecule located on the center of symmetry giving altogether four alternative orientation of the moiety. The asymmetric part of the solvent, representing a halve of the molecule, consists of two sites with refined occupancy yielding 0.69(1):0.31(1).

All major component, non-hydrogen atoms with occupancies larger than 50% were refined anisotropically. Most of hydrogen atoms were placed in calculated positions and refined within the riding model. Positions of two hydrogen atoms of urea fragment engaged in hydrogen bonds were refined. The temperature factors of all hydrogen atoms were not refined and were set to be equal to either 1.2 or 1.5 times larger than U_{eq} of the corresponding heavy atom. The atomic scattering factors

were taken from the International Tables [7]. Molecular graphics was prepared using Mercury CSD 4.1.0 program [6]. Numbering scheme and thermal ellipsoids parameters are presented at 50% probability level in **Figure S49 b)**. Packing diagrams of **2-KCl** crystal structure are shown in **Figure S50 b)**.

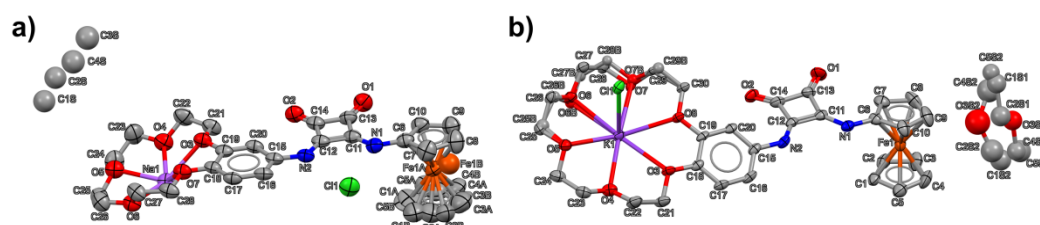


Fig. S49: Numbering scheme and atomic displacement parameters at 50% probability level for **1-NaCl** **a)** and **2-KCl** **b)** crystals. Hydrogen atoms omitted for clarity.

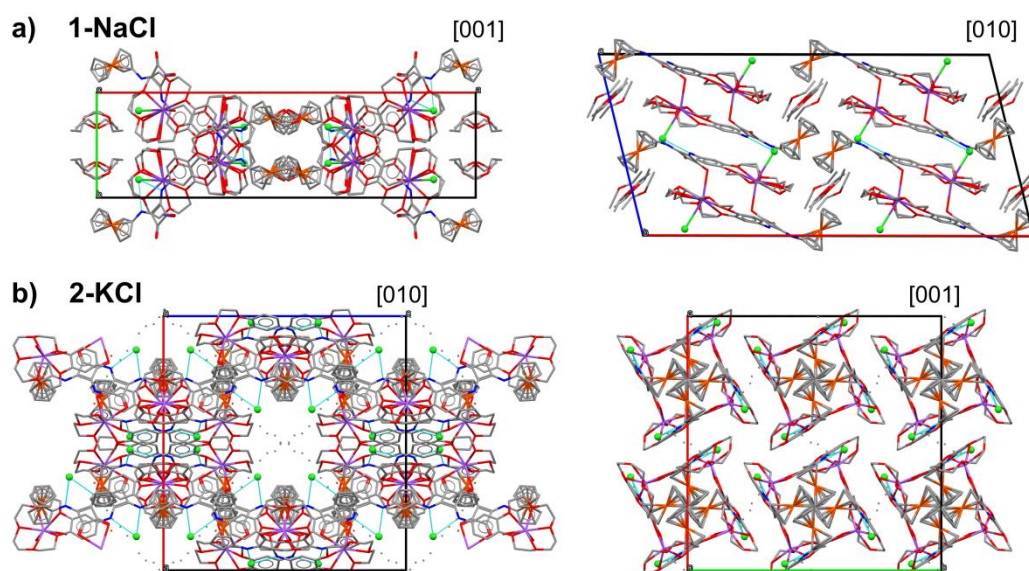


Fig. S50: Packing diagrams of **1-NaCl** viewed along [001] and [010] directions **a)** and **2-KCl** viewed along [010] and [001] directions **b)**. Hydrogen atoms omitted for clarity.

Acknowledgements

The X-ray structure was determined in the Advanced Crystal Engineering Laboratory (aceLAB) at the Chemistry Department of the University of Warsaw.

5.1. References Supplementary

- [1] APEX2, Bruker AXS Inc., Madison, Wisconsin, USA, **2013**.
- [2] SAINT, Bruker AXS Inc., Madison, Wisconsin, USA, **2013**.
- [3] SADABS, Bruker AXS Inc., Madison, Wisconsin, USA, **2012**.
- [4] G. M. Sheldrick, *Acta Crystallogr.* **2015**, A71, 3-8
- [5] G. M. Sheldrick, *Acta Crystallogr.* **2015**, C71, 3–8.
- [6] Mercury CSD 2.0 - New Features for the Visualization and Investigation of Crystal Structures; C. F. Macrae, I. J. Bruno, J. A. Chisholm, P. R. Edgington, P. McCabe, E. Pidcock, L. Rodriguez-Monge, R. Taylor, J. van de Streek and P. A. Wood, *J. Appl. Cryst.*, **2008**, 41, 466-470.
- [7] *International Tables for Crystallography*, Ed. A. J. C. Wilson, Kluwer: Dordrecht, **1992**, Vol.C.
- [8] APEX3, Bruker AXS Inc., **2017**.
- [9] SAINT, Bruker AXS Inc., **2017**.
- [10] TWINABS, Bruker AXS Inc., **2012**.